UNIVERSIDAD DE LA REPÚBLICA

FACULTAD DE INGENIERIA

Tesis para optar por el Titulo de

Magister en Ingeniería de Celulosa y Papel

EVALUACION DE CRISTALES NANOMETRICOS DE CELULOSA COMO ADITIVOS PARA MEJORAR LAS PROPIEDADES MECANICAS DEL PAPEL

(*ASSESSMENT OF CELLULOSE NANOCRYSTALS AS MECHANICAL REINFORCEMENT PAPER ADDITIVES*)

Autor: Ing. Quím. Ignacio Agustín Laborda Turrión

Director de Tesis: Dra. Maria Luiza Otero D'Almeida Lamardo

Montevideo, Uruguay

2021

TABLE OF CONTENT

c

ABSTRACT

Cellulose nanocrystals (CNC) are nanosized crystals of cellulose chains that can be extracted from several cellulose source and exhibit mechanical properties superior to Kevlar or glass fiber. These CNC were isolated using sulfuric acid hydrolysis from bleached *Eucalyptus spp.* Kraft pulp with high yield (> 70 %). CNC were successfully neutralized using a sequence of short centrifugation washing steps, drying in a transparent rigid polymer. The CNC were chemically modified at its surface prior to be used as additive to improve the mechanical properties of paper sheets. The addition of CNC obtained from three different conditions (after hydrolysis, after alkalinization and after oxidation with potassium meta periodate) were added in three levels to the paper. The results showed that acid and alkalinized CNC did not provoke a significant nor incremental increase in mechanical properties; but oxidized CNC addition results in large and continuous improvement of the mechanical properties, specially Tensile Index, Burst Index, and Folding Endurance.

KEY WORDS

D

RESUMEN

Los nanocristales de celulosa (CNC) son estructuras en el rango de los nanómetros conformadas por cadenas de celulosa empaquetadas con orden cristalino, y exhiben algunas propiedades mecánicas superiores al Kevlar o a la fibra de vidrio. Estos CNC se aislaron de pulpa Kraft blanqueada de *Eucalyptus spp*, con alto rendimiento (> 70 %). Los nanocristales fueron neutralizados exitosamente utilizando una secuencia de lavados y centrifugaciones cortas, logrando obtener un sólido que al secarse formo un polímero rígido y transparente. Los nanocristales fueron modificados químicamente en su superficie antes de ser incorporados como aditivos para mejorar las propiedades mecánicas del papel. La adición se efectuó con tres tipos de nanocristales (como se obtuvieron luego de la hidrolisis, luego de ser alcalinizados, y luego de ser oxidados por meta periodato de potasio), en tres niveles de adición. Las pruebas mecánicas sobre el papel demostraron que la adición de cristales ácidos y alcalinizados, no lograron un incremento ni significativo ni sostenido de las propiedades mecánicas. Pero los nanocristales oxidados, provocaron un aumento claro y sostenido del desempeño mecánico, especialmente el índice de tracción, la resistencia al reventamiento, y la resistencia a pliegues.

1 INTRODUCTION

The present work explores the feasibility of improve paper properties using nanotechnology. This concept has emerged as one natural extension of the many nanotechnology applications. Wood fiber, the main constituent of wood pulp used in paper, is itself a superstrucural of bottom up construction, where supramolecular and nanoscale aspects define its mechanical properties. Cellulose nanocrystals (CNC) are one of the nanosized structures that integrates the fibers, and own attractive mechanical properties. CNC isolation has been studied from different sources, using mostly (but not exclusively) mineral acid hydrolysis. The use of Kraft wood pulp as source of CNC represents a clear way for its application in paper mills where low grade pulp (*ie.* waste paper from paper machine or rejects from recycled paper) could be revalorized [1]. The addition of CNC for enhancing the mechanical properties of paper represents a potential of achieve a stronger paper using materials within the paper mill stream.

The present work study the way to achieve a direct and high yield isolation of CNC, and its effectiveness when used as additive for paper reinforcement. The isolation of CNC represents a major challenge when acid hydrolysis is used, due the need of washing steeps in order to remove acid prior to use. In the present work, a simple approach of successive centrifugation was used, in order to approach to a potential industrial application. Two post isolation chemical treatments were tested

to assess the reinforcement potential of the surface modified CNC. Modified and unmodified CNC were used in three addition levels in forming paper sheets, to later conduct mechanical measures.

The following text is divided in two sections, first a theoretical background exploration about the nanosized cellulose forms, its sources, isolation methods, and uses as reinforcement. In the second part, methods and results for the isolation and chemical modification of CNC are presented. This section also presents results of the physical evaluation of paper additivated with different amounts of CNC. Results are discussed in the light of the nano composites mechanical models.

2 THEORETICAL BACKGROUND

2.1 Cellulose as raw material

Cellulose is the most abundant biopolymer; it is available in almost all the biosphere of Earth and is virtually inexhaustible. Its sources are quite varied, comprising: bacteria, fungi, animals, and plants (native cellulose). Synthesized from carbon dioxide fixation and sunlight, makes it a potentially zero carbon footprint material and fully renewable [2]. It is water insoluble, and even maintains its semi-crystalline conformation in aqueous environments, explaining it so widespread application in nature as a strength bearer structural material [3].

Wood fibers are the main commercial source of cellulosic materials, whose main industrial destination is the paper and board industry [4].

In 1838 Anselme Payen reported that the fibrous substance of all young plants is built with a chemically defined substance, composed of glucose and isomeric with starch. This substance was named "cellulose" by the French Academy the next year. Ost and Wilkening in 1910, and Willstatter and Zechmeister in 1913, published that glucose was the solely product of the cellulose complete hydrolysis. Cellobiose was detected as the hydrolysis product of cellulose by: Franchimont in 1879, Skraup and Koening in 1913, Ost in 1913, and Freudenberg in 1921; but the position of the glucosidic link in it was elucidated by Zemplen, Haworth and Hirst just in 1927. The proposition of cellulose as a linear polysaccharide of

hexose units connected by covalent glucosidic links was first presented by Staudinger and Fritschi in 1922, but was not until 1931 that Zechmeister and Toth proved the uniformity of the glucosidic bond and the linear structure of cellulose [5].

Nowadays the chemical knowledge defined cellulose as a polydisperse linear homopolymer of β-D-anhydroglucopyranose units (AGU), where the D-glucose residues had the $^4C_1$ chair conformation. Units are linked by a β(1→4) ether link, called glycosidic bond, forming a continuous structure of six member heterocyclic with two fold symmetry about the glycosidic bond, and where carbon labeled C1 is anomeric [6,7]. Chain length are in the order of 10,000 residues, which due the symmetry along the chain are grouped in dimers called "cellobiose" [8,9]. The two chain ends presents different chemical behavior: one end is the residue that has the anomeric carbon involved in the glycosidic bond (non reducing end), and the other has the anomeric carbon free to exchange between α and β form, and thus presenting aldehyde structure (reducing end) [10]. Figure 1 presents a graphical description of the structure of the cellulose.
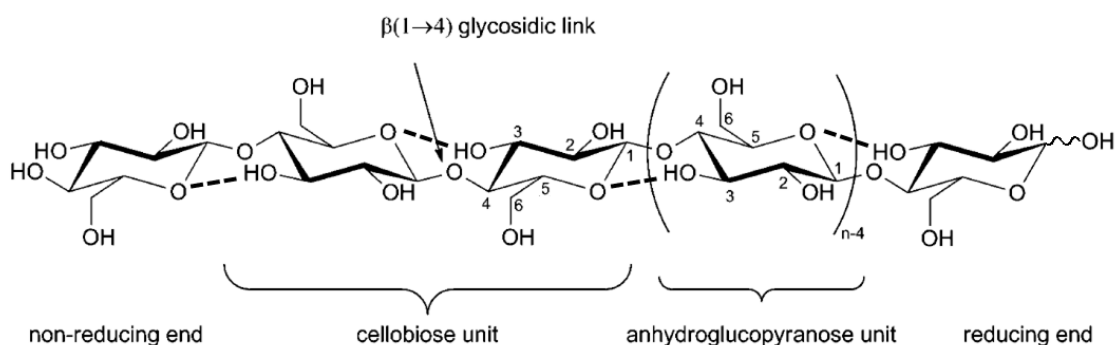

Figure 1. Representation of cellulose chain structure (adapted from [11]).

The conformation of the cellulose chain due the β linkage is a ribbon like structure, stabilized by intra molecular hydrogen bonding (dashed line in Figure 1); with oriented free hydroxyl groups that can be involved in inter molecular hydrogen bonds, giving rise to ordered arrangements [2,12]. Those arrangements promoted by hydrogen bonds and van der Waals forces form packed chains very difficult to dissolve, which acts, as the elementary building block of other hierarchical ordered structures. This bottom up construction finally form the anatomically element of the raw material source of cellulose (*eg.* wood fiber) [13].

Native cellulose chain packs in flat crystals faced up to their main crystallographic directions, with size ranging 7-9 nm width and 3 nm thick (Figure 2) [11].
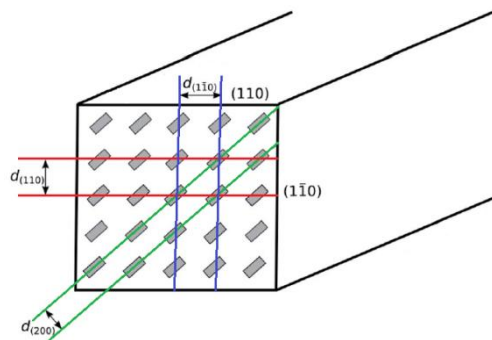
Figure 2. Model of a cellulose (type I_β) crystal with chain ends in grey, depicted with de crystallographic planes exposed at the edge of the crystal (adapted from [11]).

Those crystals are called elementary fibrils or micellar strands, and glue together by paracrystalline cellulose regions to form cellulose microfibrils (Figure 3). Those paracrystalline or amorphous cellulose are cellulose chains that have not assumed crystalline order in one section, but can be integrated in a crystal at other point [14].
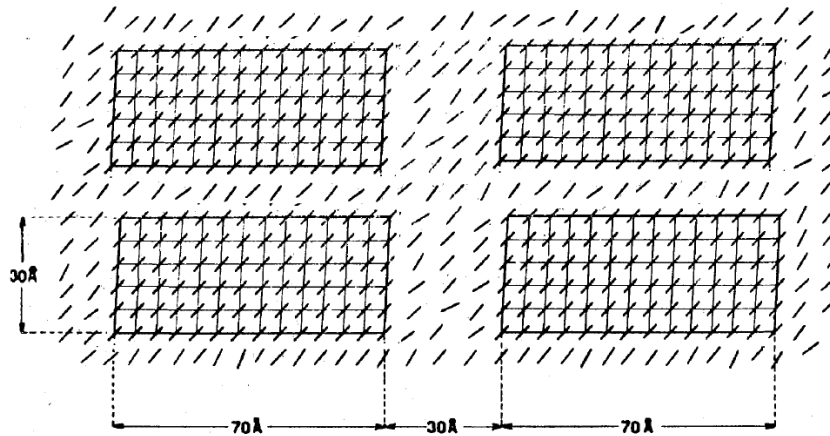
Figure 3. Model of a cross section of a microfibril composed of four elementary fibrils. Diagonal lines represent a cellulose chain ends (adapted from [14]).

Crystalline domains are interspersed with amorphous regions, and the same cellulose chain can participates in both, this is consistent with a spatial model defined as "fringed fibrilar structure" (Figure 4) [15].
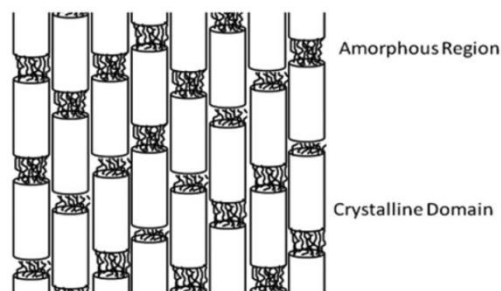
Figure 4. Model of a longitudinal section of a microfibril composed of cellulose chains bundles that alternatively form crystal and amorphous domains (extracted from [15]).

The ratio of crystalline to paracrystalline or amorphous cellulose depends on the cellulose source. The ordered alternation of crystalline and amorphous regions, results in elementary fibrils firmly held by intermolecular hydrogen bonds within the crystal, and the mechanical

anisotropy of the microfibrils. The cellulose crystal exhibits drastically different Young's modulus depending on the force direction. When stress is aligned with the main chain axis the largest values are found (206 GPa), because covalent bonds dominate mechanical response; perpendicular to this axe two smaller values are obtain, one associated with the hydrogen bond (98 GPa), and other with van der Waals forces (19 GPa) [16].

The extensive hydrogen bond net of the cellulose chains integrated in the crystals, where almost all the hydroxyl groups are engaged, makes improbable any lateral displacement or relative movement that translates in a plastic deformation [17]. The extension and distribution of the amorphous areas within the microfibrils, where the hydrogen bonding is not as extensive, define the extensibility and flexibility of the aggregate. This hierarchical structure optimized for a suited mechanical performance, scale up to superstructures that form the anatomic element of the cellulose raw material. Figure 5, depicts the different integrated structural levels for the formation of a wood fiber starting from the polysaccharide chain. This construction varies from one lignocellulosic source to other, but all of them include two other families of compounds: hemicelluloses and lignin.
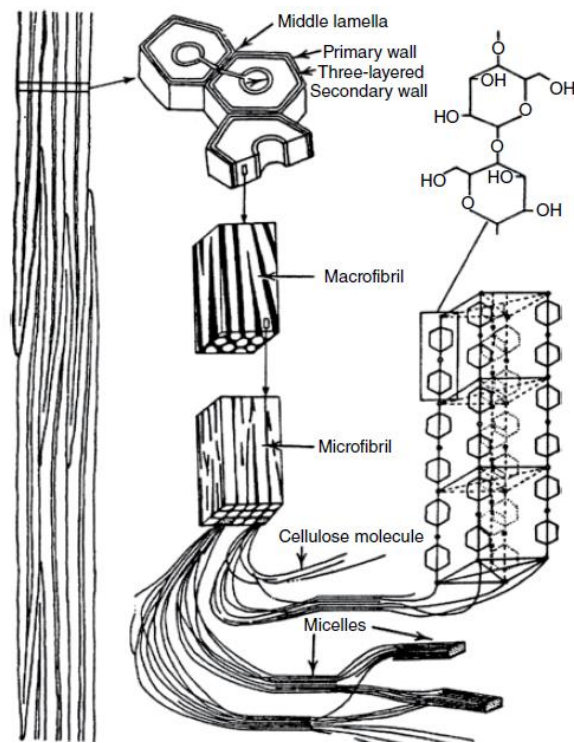
Figure 5. Model of a ultrastrucrure of a lignocellulosic fiber scaling up from cellulose chain (extracted from [17]).

This integration could be seen as a natural composite of structural and functional materials, where cellulose is the primarily but not exclusive main strength material [18]. Hemicelluloses are a group of branched polysaccharides, of amorphous structure, formed by a reduced group of monosaccharide residues, and a degree of polymerization below 300 units. Its composition varies among lignocellulosic sources and unlike cellulose they are not structural strengthening polysaccharides. Its main function is to act as a binder agent that absorbs mechanical stress avoiding microfibril breaking or splitting. Lignin is also a polymer, formed in a tridimensional extended reticulated grid of phenolic units, with not clearly defined limits in the degree of polymerization. It is originated as a byproduct of the plant metabolism, and is an important component of the

cell wall. Lignin provides mechanical rigidity to the cell wall and act as protection barrier against microorganisms attacks [19]. Lignin is degraded in acidic or alkaline conditions, like hemicelluloses; but cellulose is remarkably resistant to chemical attack or degradation. This occurs due the highly ordered structure of the crystals, causing that the inner chains are inaccessible to water and solvents. Only surface chains are accessible to reaction media. This feature makes possible that chemical pulping process like Kraft process, solubilize mostly of the lignin and some hemicelluloses, without considerable yield loss of cellulose [4].

2.2 Cellulose crystalline structure

The crystallinity of cellulose was established by Carl von Nägeli in 1858 using a polarizing microscope. Later in 1926 Sponsler and Dore, and, in 1928 Meyer and Mark, were the first to use X-ray crystallography to approach the molecular model of cellulose, but was in 1937 when Meyer and Misch using powder X-ray crystallography elucidate the first precise model for native cellulose [20,21]. Solid cellulose can crystallize in seven different allomorphs (I_α, I_β, II, III_I, III_{II}, IV_I and IV_{II}), each one presenting a different molecular orientation within the crystal, and can be differentiated by X ray diffraction [22]. The differential crystal structure drive to slightly different hydrogen bond network pattern among the chains, but the intramolecular O3H – O5 hydrogen bond is favored in all the allomorphs [23].

Type II cellulose has been reported as the most stable configuration among the seven possibilities [24]. Only types I_α and I_β are naturally occurring cellulose, and the other types are products of chemical modifications [20]. Cellulose I_α and I_β rarely occur as a pure form, I_α are the main allomorph in microorganism cellulose, and conversely I_β is the majority component of the higher plants tissues and marine animals [2]. Both types differ in the crystalline unit cell and consequently the hydrogen bond structure within the crystal, cellulose I_α exists in triclinic P_1 unit cell, whereas cellulose I_β exists in a monoclinic $P2_1$ unit cell (Figure 6) [25,26]. The existence of the dimorphism of the cellulose type I and the difference in its crystalline structures was reported in relatively recent times compared with the other polymorphs [27].
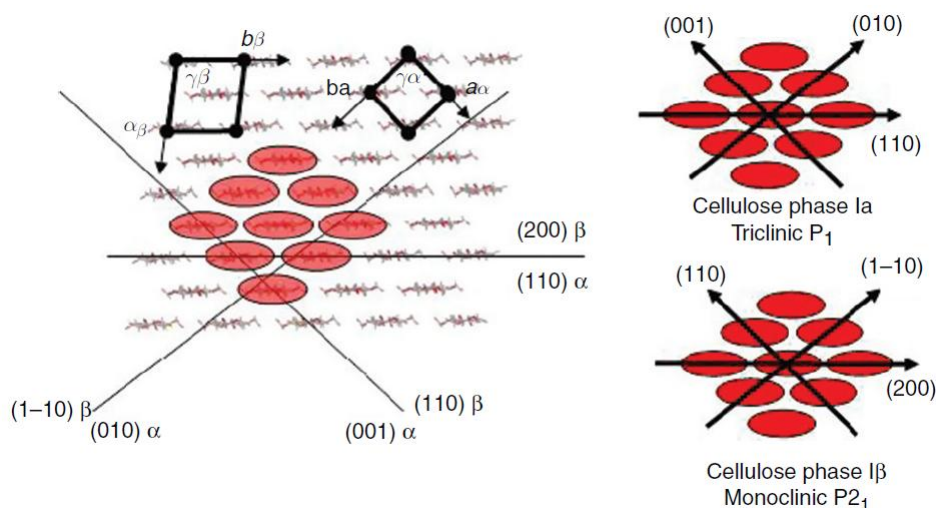
Figure 6. Crystalline arrangement of I_α and I_β cellulose, depicting their unit cells with main crystallographic directions (extracted from [2]).

Both cellulose type I crystal arrangements consist on cellulose chains stabilized in a ribbon like fashion by the O3H – O5 intramolecular

hydrogen bond, laying parallel one with another, with all the reducing ends on the same side of the crystal. Lateral hydrogen bonds between chains forms a layer structure, without clear inter sheet hydrogen bonds, making staked layers bonded only by hydrophobic interactions and weak hydrogen bonds (Figure 7) [25]. However some simulation has shown that some degree of hydrogen bonds can exists among sheets [28].
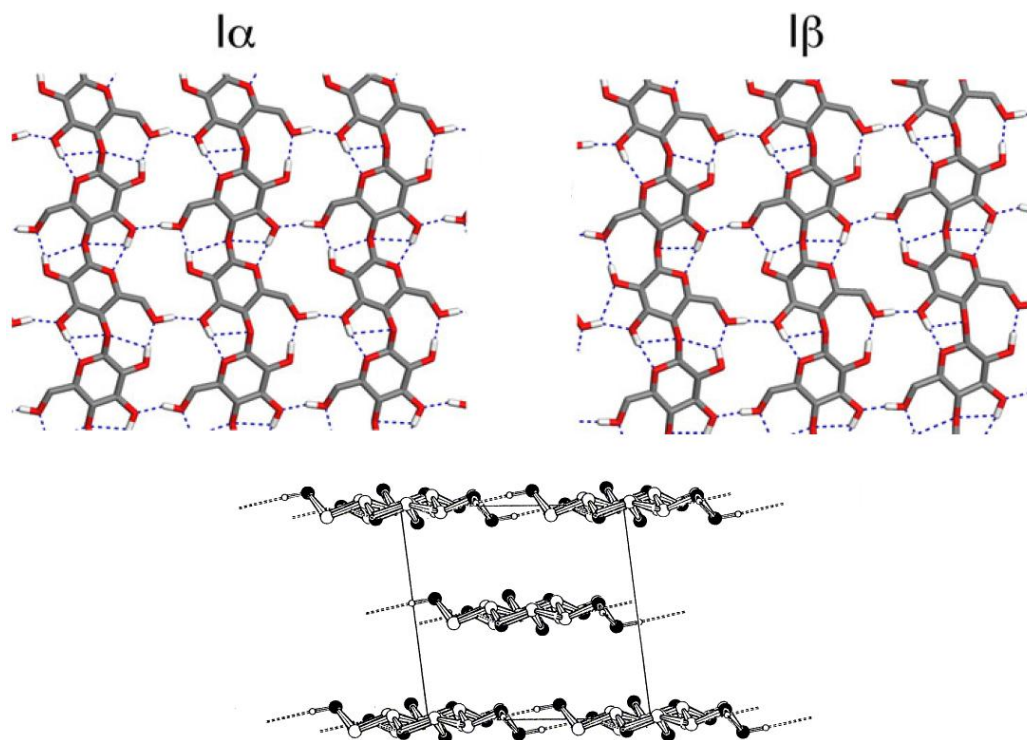
Figure 7. Crystalline arrangement of cellulose I in projections parallel and perpendicular to the chain axis, depicting in dotted line the intra and inter chain hydrogen bonds (extracted from [28,29]).

Differences among I_α and I_β lies in the alignment of the glucose residues between chains, where a relative displacement of the chains in the layer differentiate one allomorph from the other (Figure 8) [26]. It has been established that this two crystalline arrangements correspond to the two

low energy structures where cellulose chains are aligned in a parallel fashion [30].
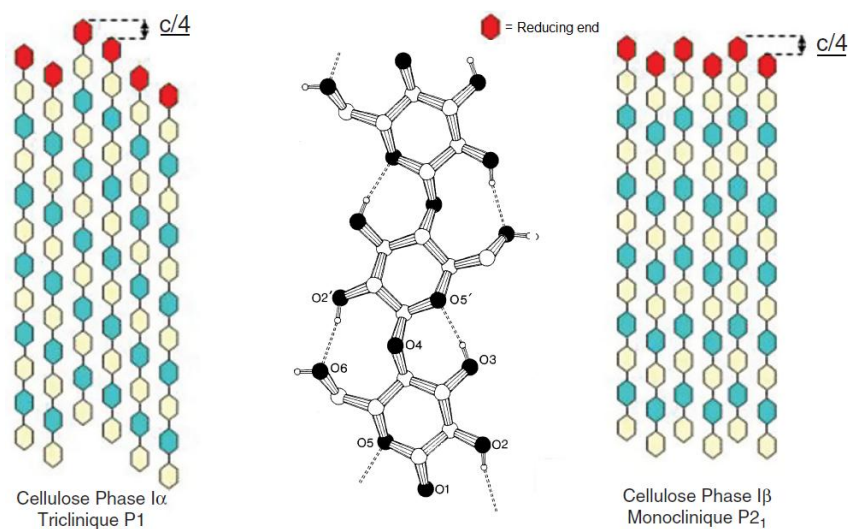
Figure 8. Schematic depiction of the chain alignment of celluloses Iα and Iβ, and the conformation adopted for the chain in both celluloses type I (extracted from [2,29]).

Industrially cellulose II is obtained from cellulose I, treating it with alkali (mercerization), or by solubilization and recrystalization (regeneration). This conversion process is well known from a long time because render better textile and paper material form native cellulose [31]. The polymorph switch is considered almost irreversible, because results in a rearrangement of cellulose chains, giving an antiparallel alignment which is a more stable structure [32]. In cellulose II chains assume the same ribbon like form that in type I, but with a different configuration in the glucose residues and aligned in an antiparallel fashion, with reducing and not reducing end alternating in each sheet (Figure 9) and packed in a $P2_1$ monoclinic unit cell [33].
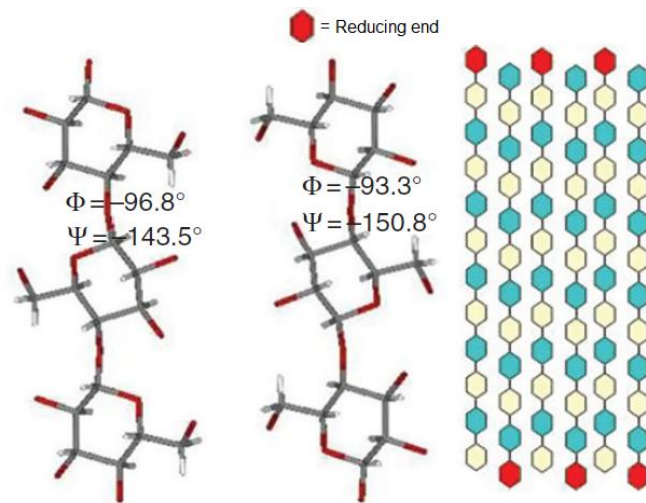
Figure 9. Schematic depiction of the chain alignment in celluloses II and the conformation adopted for the chain (extracted from [2]).

Glucose residues assumes conformation that enables the maximization of hydrogen bond formation including, unlike in type I, inter sheet bonding (Figure 10) [24,29].
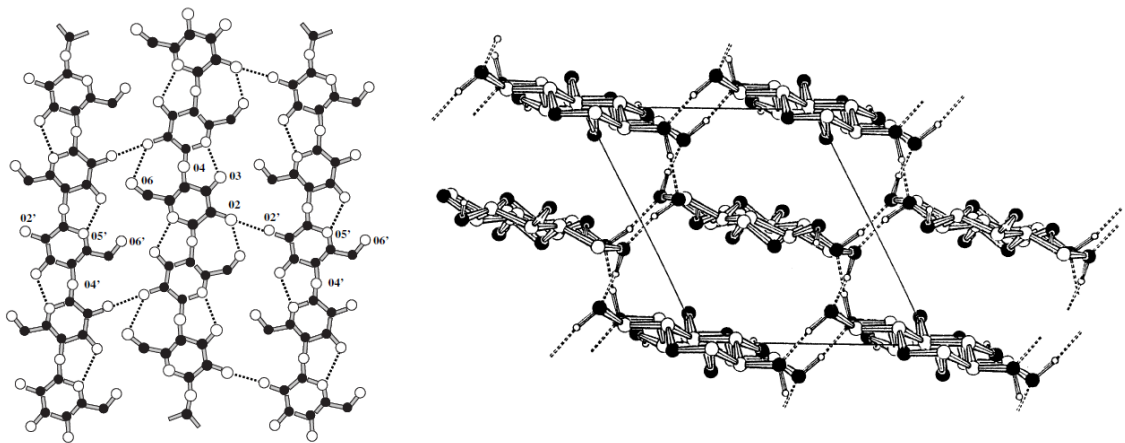
Figure 10. Hydrogen bonding between chains and among sheets in cellulose II, depicting in dotted line the hydrogen bonds (extracted from [29,34]).

As mentioned above cellulose II can be obtained by many ways, all which convert cellulose I in the more thermodynamically stable cellulose II. The

principle beneath the conversion is to enable the mobility of the cellulose chains to allow the rearrangement, and this is achieved by different paths:

_ By regeneration which is a pure physical process that consists on dissolving the cellulose in a suitable solvent, allowing total freedom of movement of the chains, following a precipitation by the addition of a non-solvent. This simple pathway has been extensively used industrially, and tailored in many ways in order to produce useful materials using native cellulose as raw material [35].

_ By mercerization, the oldest industrial pathway to produce cellulose II, developed by John Mercer in 1844. The process consists on swelling native cellulose in a concentrated sodium hydroxide solution, and then washing out the soda to obtain cellulose II. This kind of conversion can also be achieved by using nitric as swelling agents [31].

_ During the hydrolysis of cellulose by concentrated sulfuric acid, where the acid act, besides breaking glycosidic linkages, as a swelling agent and solvent. The dilution of the acidic media in order to stop the hydrolysis promotes the recrystallization of cellulose yielding cellulose II nanocrystals [36,37].

_ By directly ball milling wet native cellulose during enough time. This mechanical method allows the solid state crystalline conversion by external forces that promote the molecular rearrangement. Water content and milling time are the factors determining the extent of the conversion [38].

Mercerization is a solid state process where no solubilization takes place, and where the fibrous superstructure of the cellulose material is maintained [20]. At the chain level this process is modeled as a rearrangement promoted by the interdiffusion of sodium hydroxide used as swelling agent. Within a microfibril, the cellulose I crystals (with parallel alignment of chains) occurs in different directions, presenting an ordered array of crystals packed side by side where reducing and not reducing end are distributed in a given cross section [39]. The uptake of NaOH by these statistical distributed crystals foster the swelling of the chains within them, the disruption of crystalline order and the subsercuent diffusion of chains between crystals. Thus when the sodium hydroxide is washed out, the chains rearrange in the more stable antiparallel type II configuration [40] (Figure 11).
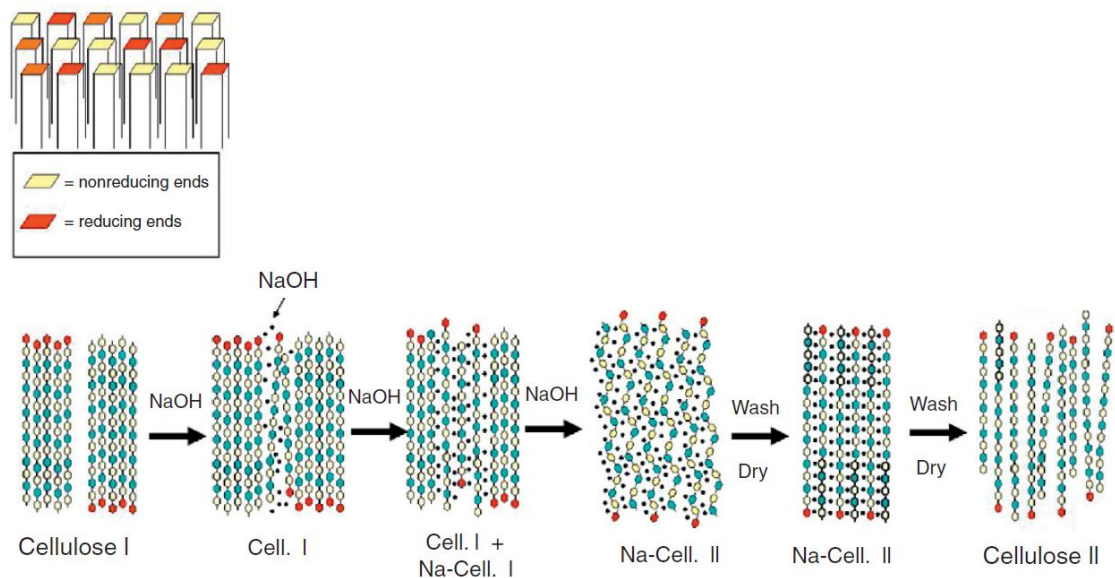
Figure 11. Schematic of the orientation of crystals within a microfibril and the steps in the crystalline rearrangement during mercerization process (adapted from [2]).

2.3 Cellulose nanocrystals isolation

According to the ISO/TS 20477:2017 standard, cellulose nanocrystals (CNC) are crystals composed of crystalline and paracrystalline cellulose where one, two, or the three external dimensions are in the 1 nm to 100 nm range. This dimensional requirement is clearly fulfill by the CNC of cellulose type II, whose ribbon like structure assure a thickness well within the range [36,37].

The first experimental approach to the isolation of the CNC from a cellulosic fibrous material were made by Nickerson and Habrle in 1947, who conducted hydrolysis with hydrochloric and sulfuric acids, and were the first to propose that the disordered intercrystalline chains sections were first attacked [41]. This approach advance the idea that the crystalline regions within the cellulosic fibers could be isolated by the selective hydrolysis or degradation of the amorphous regions between them, considering that the only difference between both were the crystal order and the resistance to hydrolysis that this implied. In 1951 Rånby confirm the feasibility of isolation of CNC producing a colloidal suspension of CNC by hydrolysis with sulfuric acid and ultrasound, reporting the electronic micrographs of the isolated CNC. It was clear then, that after the acid hydrolysis a mechanical energy input was required in order to disperse the CNC and form a stable suspension [42]. The stabilization of the suspension relies on the electrostatic repulsion of the negatively charged half sulfate esters formed in the surface, when concentrated

sulfuric acid reacts with alcohol groups of the cellulose units in the surface of the CNC [43]. The sulfonation reaction (Figure 12) has been proposed to take place on C6 of the AGU unit, despite the fact that no experimental result assessing the location of the sulfate group has been reported [11]. The sulfate esters groups represents around 1% (w/w) of the CNC bulk mass [44]. The isolation of CNC from bleached Kraft pulp by sulfuric acid hydrolysis was first reported by Revol et al. in 1992, reporting the use of this ready available source of cellulose [45].
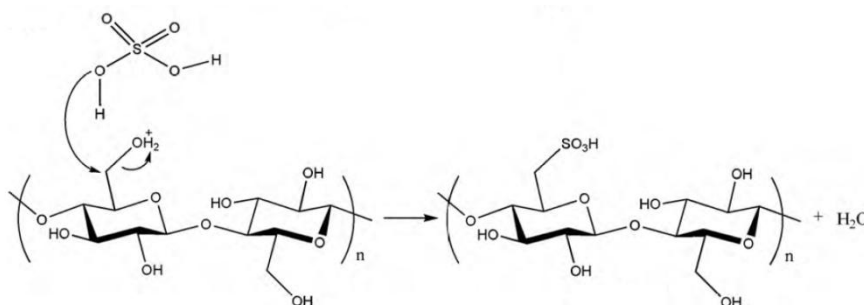
Figure 12. Sulfonation reaction during acid hydrolysis, where one water molecule is eliminated (extracted from [46]).

The properties that determine the viability of the extraction and the physical and chemical behavior of the isolated CNC are: the CNC mass yield, the size of the obtained crystals (as expression of the degree of polymerization), its crystallinity (degree and type of polymorph), and the chemical groups attached to the CNC surface [37,47,48].

Despite of being an extensively reported method for CNC isolation, the sulfuric acid hydrolysis performance involves several factors to obtain the desired result. These factors are to be optimized in order to process a

determined raw cellulose source material to CNC with the desired properties while maximizing the yield [17,37,44]. The isolation proceeds by the diffusion of the acid into the more permeable amorphous parts of the cellulosic material, where the hydronium ions can protonate the O5 of the ring, or react with the bridge oxygen in a fast equilibrium. Then one water molecule addition provokes the slow hydrolytic cleavage reaction (Figure 13). The reaction will continue at a slower rate on the reducing end of the chains integrated in the layers of the CNC. This last reaction step is tried to be avoided by stopping the reaction with a fast dilution of the acid, followed by washing steps [47,49]. The adjustment of the reaction time is critical in order to reduce the degree of polymerization to a level low enough to assure fibers were completely dispersed but not hydrolyze most of the crystalline structure [50].
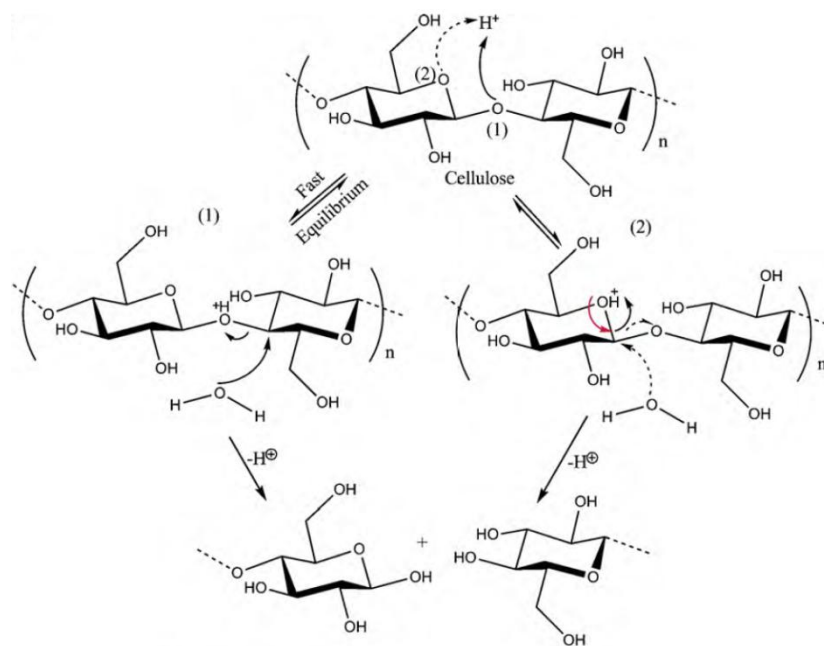
Figure 13. Two routes mechanism for hydrolysis of the glycosidic bond in cellulose (extracted from [46]).

Different cellulose sources with different pre treatments, could present very different chemical composition (types of compounds and quantities), and a different cellulose superstructure, making no possible to define an optimal universal method for isolation of CNC. Different cellulose source and different isolation processes results in CNC with different properties (specially the morphology and geometry) [47,48,51]. The optimization must overcome the complexities of the isolation system: a heterogeneous reaction media (solid: crystalline and amorphous cellulose, and liquid: acid solution), a composite material with different crystalline structure that exhibit differential chemical reactivity (amorphous cellulose between regions of crystalline cellulose), two different simultaneous chemical reactions (idealistically: hydroxyl esterification by sulfuric acid, and the cleavage of the glycosidic linkage), and the swelling and partial dissolution of cellulose chains by concentrated sulfuric acid that promotes a polymorph change [17,47].

Taking in consideration all the above factors, the concentration of the acid needs to be optimized in order to achieve a full cleavage of the amorphous cellulose while avoiding depletion of cellulose layers in the crystals, and also reach a degree of sulfonation of the crystals surface high enough to get a good dispersion of CNC [17,49]. The acid concentration is also critical in the swelling and dissolution of the whole cellulosic matrix, determining if the reactions take place in heterogeneous or homogeneous media [36,52]. Temperature is a key factor controlling the rate of:

sulfonation, hydrolysis of glycosidic linkage, dissolution of cellulose, diffusion of hydronium ion within the cellulose superstructure, and of the undesirable side reactions (oxidation and dehydration) [17,49]. Several isolation procedures using different sulfuric acid concentrations and temperatures have been reported, and in every one the temperature has been set to a constant value. To our best knowledge, there are no reports about sulfuric acid hydrolysis conducted with a settled temperature profile. Isolation of CNC from wood pulp with sulfuric acid hydrolysis is clearly straight viable routes of production, since booth are widely available commodities, but several other sources of cellulose and acids has been tested for the isolation of CNC by hydrolysis. The selection of the acid for the isolation determines the physicochemical properties of the resulting CNCs. The use of hydrochloric acid, is effective to achieve the CNC isolation, but unlike sulfuric acid the crystals are have no surface charges that stabilize them in aqueous solutions or polar aprotic solvents [53]. Other acids also used are: hydrobromic acid [54]; a mixture of citric and hydrochloric acid to obtain anionic carboxylated CNCs [55]; phosphoric acid to obtain CNCs with phosphate groups attached to the surface that due ionic repulsion form stable suspension in polar solvent and presents enhanced thermal stability (compared with sulfonated CNCs) [56]; maleic and oxalic acid to produce CNCs with carboxylic acid groups in its surface [57]; a mixture of hydrochloric with acetic acid or hydrochloric with butyric acid to produce CNCs with esterified surface [58]; a mixture of sulfuric and

acetic acid to also produce esterified CNCs [59]; phosphotungstic acid [60]; a mixture of acetic and nitric acid [61]; catalyzed formic acid [62]; and even a cationic exchange resin [63].

Reagents other than acids have been applied in isolation methods, using a diverse spectrum of cellulose sources: periodate oxidation of softwood or hardwood Kraft pulp [64,65]; the stable nitroxyl radical 2,2,6,6-tetramethylpiperidine- 1-oxyl (TEMPO) to catalytically and selectively oxidatate cellulose fibers and non wood fibers [66,67]; oxidation of various cellulosic sources by ammonium persulfate [68]; enzymatic hydrolysis of pulp [69], plasma assisted oxidation of microcrystalline cellulose [70], ionic liquid treatment of several cellulose sources including wood [71,72], subcritical water hydrolysis of microcrystalline cellulose [73]; several mechanical based processes like ball milling [74] or ultrasonication [75]. In many cases the applied process to effectively isolate CNC are combination of the before mentioned methods, in order to overcome the disadvantages presented by each method separately. The combined used of extraction methods make possible to improve the obtain CNC properties and the yield, and thus the economies of the whole extraction process [47].

A reasonable presumption is that the straightforward process for the CNC extraction utilizes microcrystalline cellulose or cellulose pulp as starting material [45,50,53,55,57,60,63,65,69,76]. However many researchers have studied the way to exploit the locally available cellulose source

(woody and non- woody plants, crops, agricultural or industrial residue) to produce a high value product like nanocellulose [77]. Some examples of this line of action are the use of: waste paper [78]; fiberboard waste [79]; mengkuang leaves [80]; banana rachis [81]; sisal [81]; kapok [81]; pineapple leaf [81]; coir [81]; guinea grass [37]; pineapple leaf [82]; coconut fibers [83]; licuri palm leaves [84]; rice straw [85]; rice husk [86]; waste sugarcane bagasse [87]; bamboo [61]; oil palm empty fruit bunch [88]; sisal [89]; cotton linter [56]; corn [90]; pomelo fruit [91]; citrus waste biomass [92]; kenaf bast [93]; jute fibers [67]; tomato peels [94]; oil palm trunk [95]; mandacaru spines [96]; cassava bagasse [97]; banana fiber [98]; grape skin [99]; flax fiber [100]; oil palm fronds [101]; potato peel [102]; sunflower stalk [103]; hemp [104]; sugarcane bagasse [105]; esparto grass [106]; garlic straw [107]; soy hulls [108]; and ramie [109].

2.4 Others nanocellulose forms

Nanocellulose is a common denomination for several types of structures, that although present the same chemical structure, they differ in morphology and production methods [110].

Deconstruction of the superstructure of the fibrous cellulose materials can produce CNC or cellulose nanofibrils (CNF). The late ones are the isolated bundles of microfibrils, composed of packed chains with alternation of crystal and amorphous domains, thus preserving amorphous parts within the structure. The most used process for this isolation are mainly

mechanical where no covalent bond cleavage of the cellulose chain is intended and only separation is procured [49]. The energy for breaking the bonds between the cellulose molecules is provided by the mechanical treatment, but can be reduced by weakening the hydrogen bond by enzymatic or chemical pre treatments [111].

Bacterial nanocellulose (BNC) is the other form of nanocellulose, where unlike the previous described nanocellulose forms, which are isolated from complex matrix, this is a chemically pure extracellular product synthesized by special bacterial strains (a bottom up process). The synthesized cellulose fibers exhibit excellent mechanical properties, non toxicity, biodegradability, and a fine structure with high degree of polymerization, but involve a high producing cost due the inherent biotechnology requirements of the process. Furthermore, extraction process does not require chemical treatments in order to remove lignin and hemicelluloses. BNC posses many applications as structural material in the medical field, making it a current topic of research in human health. Many bacterial strains and a whole spectrum of culture media have been assay to produce BNC, in order to make it commercially available [112,113].

2.5   Cellulose nanocrystals chemical modifications

CNC chemical modifications imply altering the chemical properties of the crystal exposed chains, where covalent and not covalent modifications can be applied to alter the surface behavior. This surface characteristic rules

the whole crystal interactions with other molecules [2,114]. The CNC surface needs to be modified in order to be used as compatible reinforcement in several continuous matrix (*eg.* hydrophobic polymers) without compromise the supramolecular structure; also to turn the surface more reactive to form covalent bonding; or just to produce derivatives with useful properties [114].

CNC covalent surface modifications chemistry is a natural extension of the carbohydrate chemistry in heterogeneous conditions, where the possibilities of chemical bonding are conditioned by the sterical hindrance of the crystal structure that expose a limited number of reactive groups, and the natural reactivity exhibited by each exposed group (OH group at C6 is more reactive than the others OH groups). Nevertheless the accessibility of the reactive groups is conditioned by the extension and type of crystalline arrangement, where amorphous regions are more exposed to chemical attack; and by the use of swelling agents that renders reaction media homogeneous through partial dissolution of CNC [2,114].

The spectrum of covalent modifications occurs mainly in the hydroxyl moieties; where one hydroxyl group act as primary alcohol and other two as secondary alcohols; but also other parts of the chain can suffer alterations [114]. Figure 14 schematizes the possible reactions sites within the chain. Considering that the CNC have a surface area in excess of 300 m^2/g, results in 2–3 mmol/g of surface hydroxyl groups for chemical reactions, enabling attach any desired functionality to the surface of the

AGU unit [115]. Some of the most reported covalent modifications are: esterification [58], acetylation [116], acylation [117], cationization [118], silylation [119], carbamination [120], TEMPO oxidation [66,67], periodate oxidation [121–124], and copolymerization grafting [125]. Exists many other reported reactions that exploit the hydroxyl reactions path [11,114]. Besides covalent modifications, CNC surface can be modified by non covalent reaction, but by physical interaction or adsorption of molecules, mostly of them surfactants or macromolecules, which change the hydrophilic natural affinity of the CNC to hydrophobic [126].
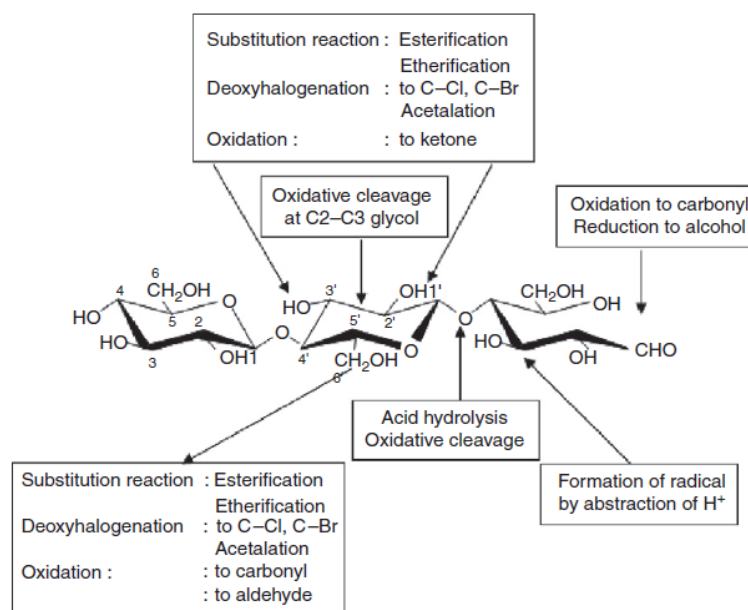
Figure 14. Cellulose position for chemical reactions (extracted from [2,127]).

When isolated by sulfuric acid hydrolysis, CNC underwent *in situ* esterification reaction, where the surface is spotted by sulfate esters. This starting modification, conditioned the behavior of the CNC in several ways:

imparts an electrostatic stability to the CNC in water suspensions avoiding agglomeration due repulsive negative charges, makes CNC more hard to retain during sheet forming, and the sulfate esters groups can be cleaved from surface releasing sulfuric acid that can promote further degradation reactions [17,43,49]. Thus the elimination of the effects produced by sulfate groups previous the use of CNC has been regarded as necessary, and has been achieved via desulfonation (de-esterification) by heat or neutralization by alkali (producing the salt form) [17]. Removal of the sulfate by heat exploits the fact that the sulfate esters groups undergo hydrolysis in acidic media, followed by a washing step [46,50]. The alkalinization or neutralization uses a basic salt (eg. sodium bicarbonate or sodium hydroxide) to bring a counterion that renders neutral the sulfate ester group [52,109,118,128,129].

The presence of multiple potential reactive sites makes cellulose a substrate of a broad spectrum of possible products, depending on the oxidizer, the reaction conditions, and the cellulose form. Among the oxidizing agents, two classes exist, selective and non-selective, where the already mentioned TEMPO and periodates belongs to the first one. In both cases, besides its use to achieve CNC isolation, the reaction that takes place selectively introduces reactive group that permits easily introduce covalent modifications [2,123,130]. TEMPO converts hydroxyl at C6 in carboxyl, and periodate oxidize the vicinal hydroxyl groups at C2 and C3 in two vicinal aldehyde groups [121,124]. Figure 15 depicts the overall

reaction and mechanism of periodate oxidation, where one periodate ion form two aldehyde functionalities on a AGU releasing one iodate ion [131].
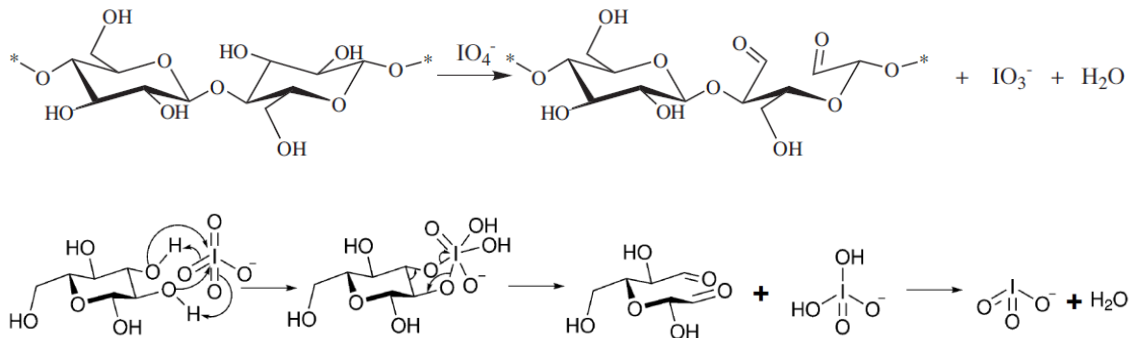
Figure 15. Reaction and mechanism of periodate oxidation (extracted from [11,123]).

Without further modification aldheyde groups are prone to generate new covalent bonding reacting with hydroxyls present in other cellulose chains. The formation of acetal and hemiacetal linkages among oxidized groups in CNC surface and other groups present in CNC or in fibers, form a covalent cross linking, and thus acting as a binding or reinforcement additive when added to cellulose fibers. This effect is schematized in Figure 16, and is the principle laying behind the paper wet strength improvement [122].
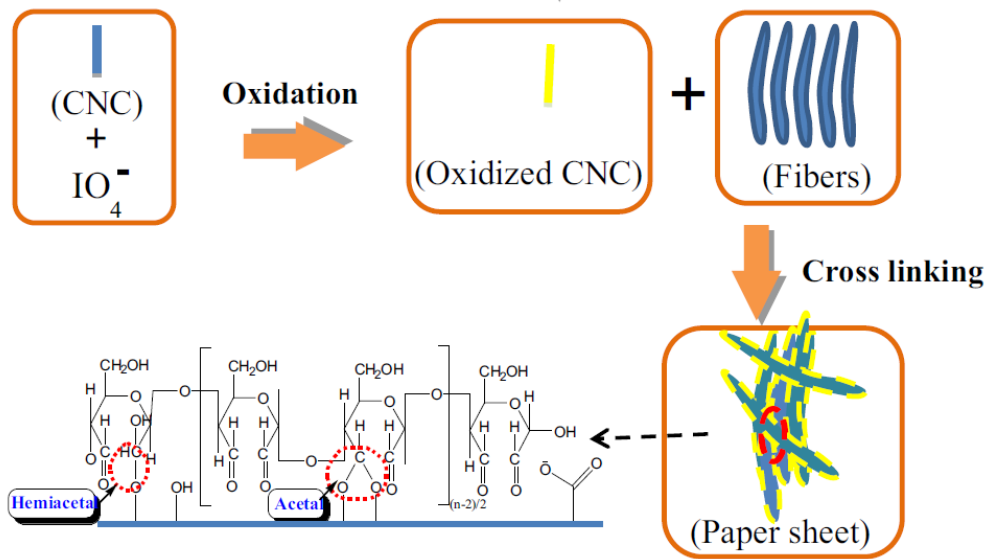
Figure 16. Crosslinking of oxidized CNC with fibers (adapted from [122]).

2.1 Cellulose nanocrystals as paper additive

Paper additives are classified into two major families, the process aid and the properties enhancers. The first ones are intended to improve the efficiency and optimize the result of the forming process, but do not impart any specific property to the resulting paper. The late ones are those which CNC belongs, additives that contribute with tailored and desirable properties to the final paper product [132]. Addition of nanosized materials has the advantage of the high surface area / weigh ratio, achieving a high impact effect in all the applications where the interface contact between additive and matrix play a critical role [15,133]. The nanoadditives could be of diverse nature, but one of the most interesting courses of action is the incorporation of those generated from the side stream of pulp production, like CNC, to be used as mechanical reinforcing agent. This

28

aspect generates much interest due to the fact that CNC from traditional sources posses a cost superior to other commercial strengthening agents [134].

The addition of CNC to paper pulp has excellent compatibility due to its same origin, and enables a homogeneous mixture, tackling one of the most prominent problems when using CNC as polymer composite reinforcement. The high compatibility with the base material and the abundance of reactive hydroxyls groups on the surface, makes possible a broad range of chemical modifications to tune the crystal physicochemical properties [31,114,133]. This feature enables the modification of the properties of a paper by the addition of a compatible nanostructure additive carrying the desired properties, avoiding the chemical modification of the whole matrix. The nanocrystals can undergo modification of their surface without affect crystal morphology or integrity. Different surface modifications have been studied with the sole purpose to increase the mechanical performance of matrixes, where modified nanocellulose additives has been added, obtaining in some cases significant improvements of the paper mechanical properties [17,31,47].

The addition of cellulose based nanoadditives to improve the mechanical performance of paper can be achieved by two ways: a physical reinforcement effect provided by the large surface area of the nanocellulose, where multiple hydroxyl groups form hydrogen bonding with the fiber network; or by the covalent bonding of modified surface

groups in nanocellulose with the fibers [135]. The physical reinforcement mechanism relies on the increase of the density of hydrogen bonding in the paper, similar effect that is produced by the increase of the fines due beating or refining. The reduction of porosity and the increase of drain time are concomitant effects [132,136,137]. The entanglement of the nanocellulose, although does not cause a significant effect in paper matrix due to the chemical similarity with the matrix, can lead to an increase in the mechanical properties of the paper. For this reason the CNF that have greater ratios between its length and diameter, are preferred in this scenario of reinforcement [89,134]. CNF typically exhibit aspect ratio from 15 to 100, and for CNC ranges from 1 to 100, where the mode of isolation and origin are determining factors [138]. The CNC with smaller ratios between its length and diameter are unable to entangle, which is a disadvantage compared to CNF with higher ratios, but on the other hand they have larger crystallinity and more uniform structure that make them exhibit impressive mechanical properties [31,110]. To this, can also be added that they have Young's modulus (70-166 GPa) comparable with Kevlar (60-125 GPa), and density (1.5-1.6 $g.cm^{-1}$) quite below glass fiber (2.6 $g.cm^{-1}$) [15,17,47]. These advantages must be exploited by making them anchor in the fiber network by covalent bonding [122].

3 EXPERIMENTAL

3.1 Objective

The objective of the research was to assess the use of cellulose nanocrystals as additives for improve the mechanical properties of paper. The CNC were isolated and used procuring a direct approach that reduces the process steps to a very minimum. Isolation aim to maximize yield while maintaining high crystallinity, and whisker like morphology of CNC. The alteration of paper properties were evaluated after the addition of three kinds of CNC: acid (as obtained), oxidized, and alkalinized. No additives were used to help in the paper forming process, neither dispersion agents to improve CNC mixture, in order to visualize the solely effect of CNC addition.

3.2 Materials and methods

3.2.1 Cellulose nanocrystals isolation

The CNC isolation was achieved from *Eucalyptus spp.* bleached Kraft pulp (UPM Fray Bentos Mill) by acid hydrolysis. The water content in pulp was approximately 66 % (w/w), wet base.

The pulp was dissolved in H_2SO_4 70 % (w/w) (Merck EMSURE® ISO) with a pure acid/dry pulp ratio of 16 (w/w). The dispersion of the pulp was carried under ice bath and mechanical stirring, using a commercial kitchen

immersion hand blender (2 inches stainless steel blade, output power 600 W) for 10 minutes. Then the ice bath was removed and the mixing continued for another 10 minutes at room temperature. The appearance of the reaction mixture was of an ivory opaque gel. The hydrolysis reaction was stopped by diluting the reaction mixture with two times its volume of distilled water. The dilution was performed with magnetic stirring under ice bath. The resulting was an opaque white suspension that was centrifuged (3000 rpm for 2 min), and the supernatant discarded, the pellet was resuspended in distilled water. This process was repeated two times for a gross acid elimination. The pH of the suspension was strongly acid (pH≈1) (Merck MQuant® pH indicator stripes).

3.2.2 Cellulose nanocrystals suspension neutralization

The acid suspension of CNC was repeatedly (6 to 8 times) centrifuged (3000 rpm for 2 min) in order to remove the remaining acid. After each centrifugation, the clear supernatant was discarded and the remaining pellet and solution resuspended again in distilled water. The process was concluded when the clear supernatant reach a pH value of approximated 6.

3.2.3   Dry weight determination

The dry matter content of cellulose pulp and neutralized cellulose CNC suspension were determined using "Moisture Balance HA60" (Precisa Gravimetrics AG – Switzerland) at 112 °C until reach constant weight. Acid cellulose nanocrystals suspension dry weight was determined using the same procedure, after neutralization by repeated centrifugation as described before.

3.2.4   Cellulose nanocrystals oxidation

Acid suspension of CNC presenting 16.2 dry grams per liter was oxidized using a saturated solution of potassium meta periodate (Merck Sigma-Aldrich) during all the reaction length. The reaction was performed in dark, with magnetic stirring, for 4 hours at 30 ºC. The final suspension was decanted to remove undissolved crystals of potassium meta periodate, and used without further processing.

3.2.1   Cellulose nanocrystals alkalinization

Acid suspension of CNC presenting 5.6 dry grams per liter was treated with sodium hydroxide (Fluka Honeywell) at a concentration of 13 g for each gram of CNC present in suspension. The reaction was performed at 50 ºC for 5 hours, with magnetic stirring. The final suspension was used without other processing.

3.2.2 Laboratory sheet formation

Laboratory sheets were formed with the addition of different amounts of CNC. The sheets were formed with refined and not refined pulp. The sheet forming procedure was according standard ABNT NBR ISO 5269-1. The equipment used was a "*Formador de Folhas FQ-21*" (Regmed-Brazil). When required *Eucalyptus spp.* bleached kraft pulp (Votorantim Celulose e Papel) was refined in PFI mill according standard ABTN NBR 5264-2. The mill used was the "P.F.I.-MILL Nº241" (HAMJERM-Norway). Drainabilty of pulp by Shchopper-Riegel method was measure according standard ABNT NBR 14031. The equipment used was a "Schopper-Riegler Pneumatic model SR/P" (Regmed-Brazil). Laboratory sheets were all formed at a base of approximately 60 g/m^2 using refined and not refined pulp, and supplemented with different amounts of CNC suspensions over the base quantity of pulp. The sets of laboratory sheets formed are detailed in Table 1.

Pulp and kind of CNC added	Percentage added of CNC (w/w both in dry basis)			
	0 %	2.5 %	5 %	10 %
Not refined pulp + Acid CNC suspension	8 laboratory sheets	8 laboratory sheets	8 laboratory sheets	8 laboratory sheets
Refined pulp + Acid CNC suspension	8 laboratory sheets	8 laboratory sheets	8 laboratory sheets	8 laboratory sheets
Refined pulp + CNC oxidized	--	8 laboratory sheets	8 laboratory sheets	8 laboratory sheets
Refined pulp + CNC alkalinized	--	8 laboratory sheets	8 laboratory sheets	8 laboratory sheets

Table 1. Laboratory sheets formed in each level of supplementation and type of base pulp

The different CNC suspensions were mixed with the base pulp during the disaggregating phase of the sheet forming. The disaggregation took place at 30000 revolutions in a pulp disintegrator "*Desintegrador modelo OSE 3000*" (Mecatécnica Indústria de Aparelhos de Medição – Brazil).

3.3 Characterization

3.3.1 Physical test of the laboratory sheets

The determination of physical properties was conducted according standard DIN EN ISO 5270:2012. The measured properties were: grammage, thickness, tensile index, tear index, burst index, air permeance and folding endurance. Grammage was determined using a balance scale model "P 1210" (Mettler – United States). Thickness was determined using a paper thickness gauge "ESP/PM-M" (Mecatécnica Indústria de Aparelhos de Medição – Brazil). Tensile properties were determined using a tensile test machine "DL-500" (Emic – Brazil). Tear index was determined using an Elmendorf tear tester model "ED-160" (Regmed-Brazil). Burst index was determined using a bursting strength tester model "MTA-2000" (Regmed-Brazil). Air permeance was determined using a Gurley high pressure densometer model "PAG-100" (Regmed-Brazil). Folding endurance was determined using a folding endurance tester model "M.I.T." (Tinius Olsen Testing Machine Co. – United States). To perform the determination of physical properties, the laboratory sheets

were conditioned and tested under the controlled atmosphere indicated in the standard ISO 187:1990.

3.3.2 Fourier-transform infrared spectroscopy (FTIR)

Aliquots of acid CNC suspension, oxidized CNC suspension, and alkalinized CNC suspension, were washed by five cycles of centrifugations (3000 rpm for 2 min), supernatant removal, and pellet resuspended in water. After that the samples were dried at room temperature for 5 days. Infrared spectra were acquired using a Thermo Fisher Scientifica Fourier Transform Infrared Spectrometer, Model Nicolet iS10. Infrared spectra of the pulp used as raw material was also measured, using pulp oven dried at 105 °C until constant weight.

3.3.3 X-ray diffraction (XRD)

Neutralized CNC suspension was oven dried at 120 °C up to constant weight, and the solid residue milled to powder and sieved in a 325 mesh screen. XRD measurements were carried out on a X-ray diffractometer Shimadzu 6000. The patterns with Cu Kα radiation ($\lambda K\alpha 1 = 0.154060$ nm) at 45 kV and 40 mA were recorded in the region of 2θ from 5 to 70° at a scanning rate of 2°/min.

3.3.4 Scanning Electron Microscopy (SEM)

Aliquots of acid CNC suspension were washed by five cycles of centrifugations (3000 rpm for 2 min), supernatant removal, and pellet resuspended in water. After that, the samples were dried at 25 °C and 50 % relative humidity for five days over glass plate. Specimens were covered with a thin layer of gold and palladium for microstructural analyses using a Quanta 650 FEG microscope (Thermo Fisher – United States). The scanning was carried out under a voltage of 20 kV in secondary electrons mode.

3.4 Results and discussion

3.4.1 Cellulose nanocrystals isolation

Reported hydrolysis of bleached *Eucalyptus* pulp to obtain CNC typically uses acid concentrations around 64 % (w/w) and temperature of 45 °C [48,50,139]. In the present work the acid concentration used was slightly higher (66 % w/w). The objective was to foster an extensive hemicelluloses and non crystalline cellulose hydrolysis; avoiding the crystalline cellulose degradation and thus achieve a CNC isolation yield close to the theoretical limit for chemical pulps (around 70 %) [17].

The two key factors affecting the reaction development are: acid concentration and temperature of reaction, where time of reaction media and mechanical stirring are less critical. Acid concentration ranging from

64 to 70 % (w/w), affects drastically the hydrolysis performance, because swelling and solubility of the cellulose occurs in a large extent. This effect causes that hydrolysis and regeneration (in cellulose type II) takes place simultaneously. The regeneration of cellulose implies: loss of yield, the reduction of the degree of polymerization of crystals, and its change of morphology (from large needle like crystals to short rounded points) [36,37,52]. The same acid concentration used in the present work (66 % w/w), was reported in the isolation of CNC where type I, type II, and a mixture of both polymorph were obtained [36]. Acid concentration values over 70 % (w/w) have shown a fast dissolution and hydrolysis of cellulose, leading to a full conversion to water soluble oligomers and negligible yields, even at 25 °C [52,140]. Conversely acid concentration under 64 % (w/w) results in a not extensive hydrolysis of the amorphous cellulose, and low level of sulfonation, hampering thus a good isolation and dispersion of cellulose crystals. The degree of sulfonation of CNC has been marked to be solely dependent of the acid concentration [141].

Temperature of the hydrolysis reaction media has shown an effect in the polymerization degree (directly affecting crystal size), and in the yield of the isolated CNC at low acid concentrations, but at higher acid concentrations the effect is not appreciable. At low concentrations the temperature promotes, first the cleavage of non crystalline cellulose, reducing the polymerization degree, and then the increase in the degree of sulfonation of the isolated crystalline cellulose, causing more solubilization

of the crystals and consequently less yield [141]. The present study was conducted under the supposition that the optimal temperature condition for the isolation was a two stages temperature profile. First stage carried on ice bath, to control the exothermic effect of the acid dissolution by the pulp humidity, and to allow a homogeneous dispersion of the pulp. Then a second stage, where the ice bath is removed, and the reaction continue at room temperature reaching up to 18-20 °C. Is in this second stage where the most of the hydrolysis take place. When the temperature was allowed to rise over 30 °C the result was the complete hydrolysis of the pulp driving to a negligible CNC yield.

After the hydrolysis degrades the amorphous cellulose, reaction time is not a determining factor for the quality of the CNC due to the slower rate of hydrolysis of crystalline cellulose. Nevertheless long reaction times allow more crystal degradation lowering the CNC sizes [47,77]. Also extended times allows that oligomers and monomers undergo side reactions like dehydrtatation, that turns the reaction media brownish [17]. After 25-30 minutes of reaction it was evident a sharp decrease in the viscosity of the reaction mixture, probably due the extensive loss of amorphous cellulose chains, but a possible dissolution effect cannot be discarded due the high acid concentration used [41].

Stirring of the reaction media was used to ensure a homogeneous contact between the acid and the pulp, prompting a fast dispersion and full dissolution of the pulp, and to help through mechanical energy input the

cleavage of amorphous cellulose chains. Despite the fact that the sulfate groups in the surface of the CNC induce electrostatic repulsion and stabilization of the suspension, Van der Waals bonds need still to be broken to attain a good CNC suspension [11,52].

Magnetic agitation was not possible due the high viscosity of the reaction media, especially at the beginning of the reaction, when the rheological behavior of the reaction mixture was of a thick gel.

At the end of the hydrolysis an aliquot of the reaction volume was diluted to stop reaction, and then neutralized by successive centrifugations, reaching a pH≈5. The resulting suspension was oven dry at 105 °C producing an isolation yield of 71 % (dry CNC of dry pulp). This value was close to the theoretical limit and above the yield reported (65 %) for CNC isolated from bleached *Eucalyptus* kraft pulp [48]. No significant decrease in yield was observed as it would be expected due the high acid concentration used, but this is aligned with what has been reported for short hydrolysis times [37,52]. The straightforward use of centrifugation cycles after hydrolysis showed to be a viable route in order to remove most of the acid of the NC suspension, not requiring the use of dialysis under continuous water flow for neutralization. This change in methodology significantly reduces the time and materials required for neutralization. This approach has been reportedly used in the isolation of CNC from microcrystalline cellulose [116]. The major drawback of this technique is the inability to remove the acid molecules trapped in the

bound water layer surrounding the CNC, whose concentration is governed by a diffusion process to the bulk media [17].

A portion of the acid suspension obtained from the hydrolysis was centrifuged, and the pellet, which presents a white gel appearance and a consistency of ≈ 30 % (w/w), was dried at room temperature (Figure 17). The aspect of this CNC gel was well according to what has been reported by other authors [76].

Figure 17. Gel obtained by drying at room temperature of acid CNC suspension

3.4.2   X-ray diffraction (XRD)

XRD pattern of the CNC suspension (Figure 18) shows a diffraction pattern corresponding to cellulose type II polymorph. The three characteristic peaks of this cellulose type have Miller indices of (1-10), (110) and (020), corresponding to 2θ values of 12°, 20° and 22° respectively.

The profile correspond more to a random crystallites orientation, than with an orientation along fiber axis [142]. The transition of cellulose type I corresponding to the Kraft raw pulp to the polymorph II has also been seen in previous reports of isolation of CNC from *Eucalyptus* kraft pulp [139]. The dissolution of cellulose Type I with concentrated sulfuric acid (over 64 % w/w) trigger the rearrange in the crystalline network, so when diluted with water it precipitated the type II polymorph of crystalline cellulose [52]. Similar spectra were reported as pure type II in a research where samples of CNC of type I and type I + II were also measured and compared [36].

The crystallinity of the CNC suspension, defined as the crystalline fraction of the whole mass of material isolated, was not possible to determine easily from the diffraction spectra, because most of the methods are envisaged for type I cellulose [143]. In the present work the relation between the area of the three distinctive peaks of Type II cellulose and the total spectra area was used as crystallinity ratio [51]. The actual value was around 73-75 %, close to those reported for CNC Type I isolated from *Eucalyptus* pulp [48], and in good agreement with values reported when the same dilution processes (in order to stop the reaction) were applied [37]. This result, below the expected crystallinity for the pure isolated CNC (>90 %), is a consequence of the hydrolysis conditions. A very aggressive acid hydrolysis as used in the present work is intended to achieve: an extensive sulfonation of cellulose chains, a complete dissolution of CNC, a

full cleavage and solubilization of hemicelluloses and amorphous cellulose, and thus maximizing CNC yield and crystallinity.
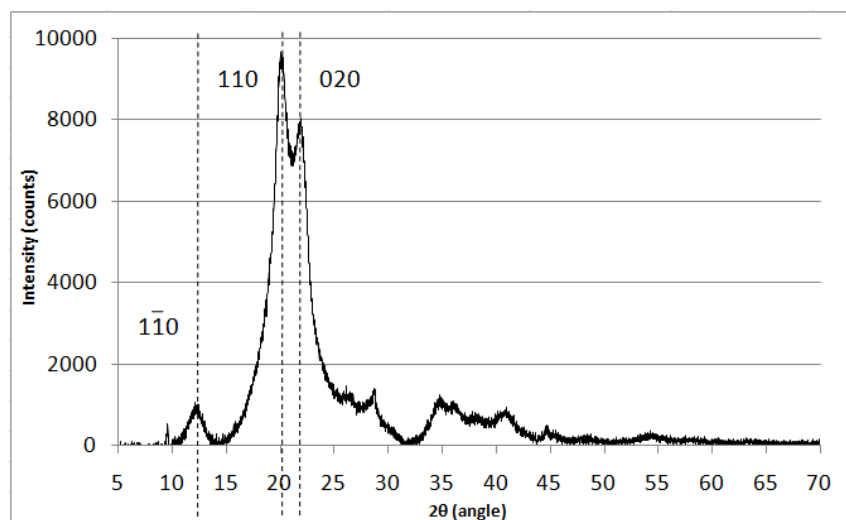
Figure 18. X-Ray diffraction pattern of CNC

3.4.3   FTIR spectroscopy

FTIR spectra of all the CNC types are shown in Figures 19 to 22. Cellulose exhibit a set of typical bands in the range $800 - 1650$ cm^{-1}, but the peaks assignments is not easy due to the peak overlapping, and because several vibrational bands corresponds to coupled motions of groups and bonds. Assign one band to a certain vibration type of a group is rare in this kind of matrix. Table 2 details the IR peak assignement for: the bleached Kraft pulp used as source for nanocelulose isolation, and for the neutralized, alkalinized and oxidized nanocelulose samples. Many authors make different band assignments, occasionally contradictory, while others just make assignment to different regions in the molecular structure, based

on observation of several samples spectral data [144–147]. Example of this is the peak corresponding to the "anomeric region"; β-linkage band at about 900 cm^{-1} distinguish from α-linkage band located at small wavenumbers [146,148]. In the region comprising from 950 to 1120 cm^{-1} the maximum absorption bands are found. This bands, characteristics of cellulose arise from the overlapping of the majority of the C-O stretching vibration, with contribution of some C-C, C-H and C-O-C motions [147–150].

As expected the IR band characteristic of hemicelluloses at 1750 cm^{-1} is present in the pulp spectra, but is not present in the nanocelullose samples, due the acid hydrolysis effect on this more labile polymer, that undergo degradation faster than crystalline cellulose. In all the nanocellulose samples spectra, are still present the cellulose peaks, implying that the cellulose were not degraded or eliminated during the acid hydrolysis and the subsequent chemical modifications. Sulphate esters groups (-O-SO3Na) peak at 1130 cm^{-1} were not detected in the neutralized nanocelulose sample, this limitation has been reported early, where a high degree of sulfonation (around 150 sulfate groups per 100 anhydroglucose unit) is require to allow IR detection [17]. Other limitation arise in the determination of aldehyde moieties in C3 and C5 after periodate oxidation; the residual amount of water reacts reversibly with aldehyde forming OH groups, which cannot be differentiated by IR absorbance from already present hydroxyls [151].
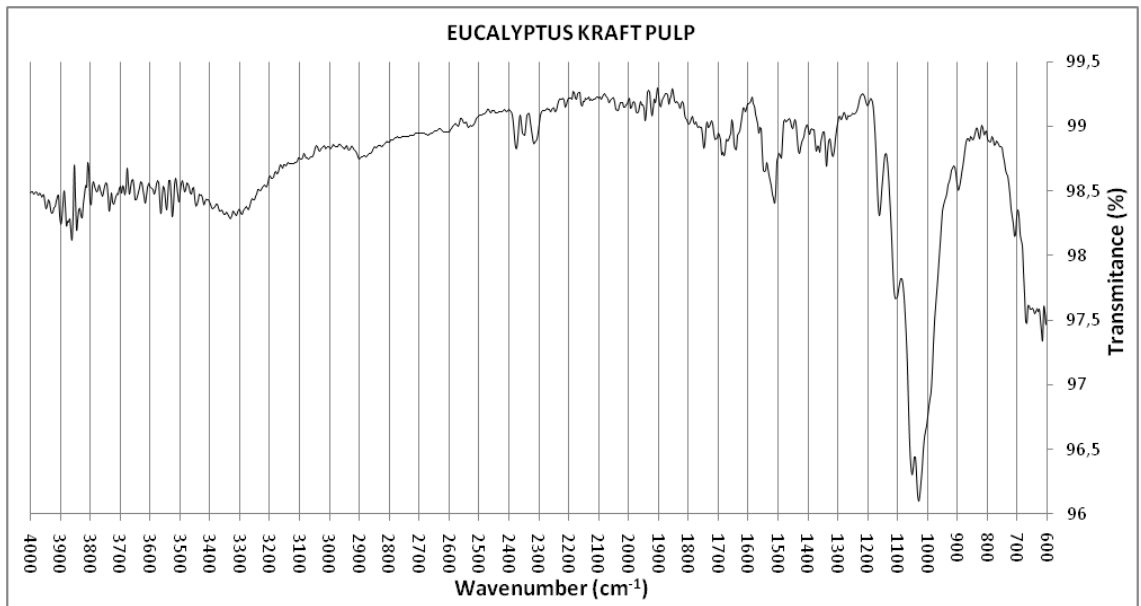
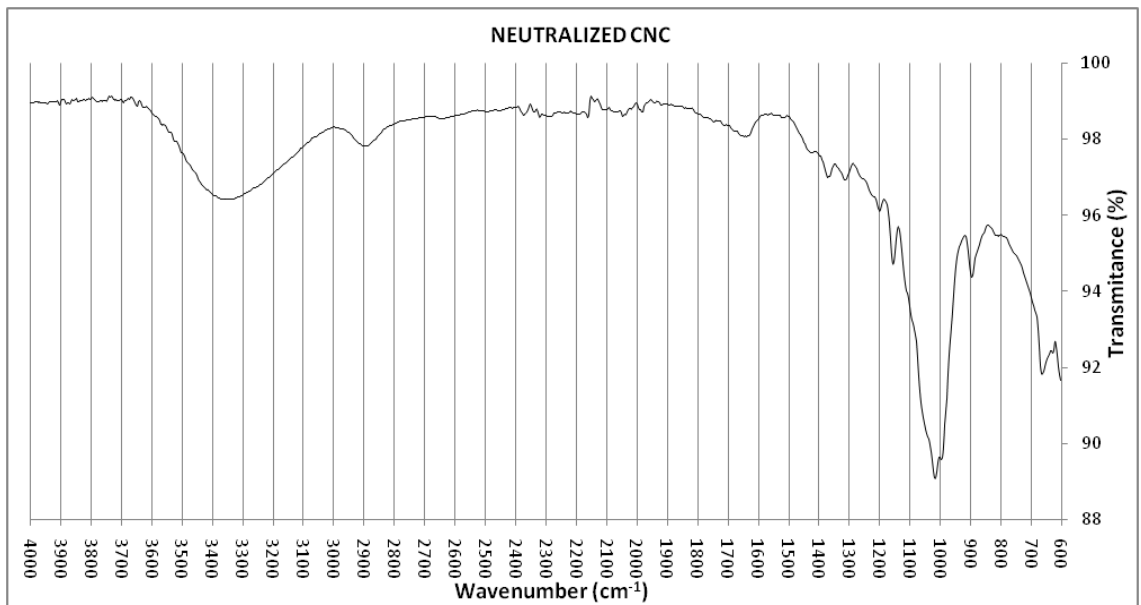Figure 19. FTIR spectra of the raw pulp used as source of CNC

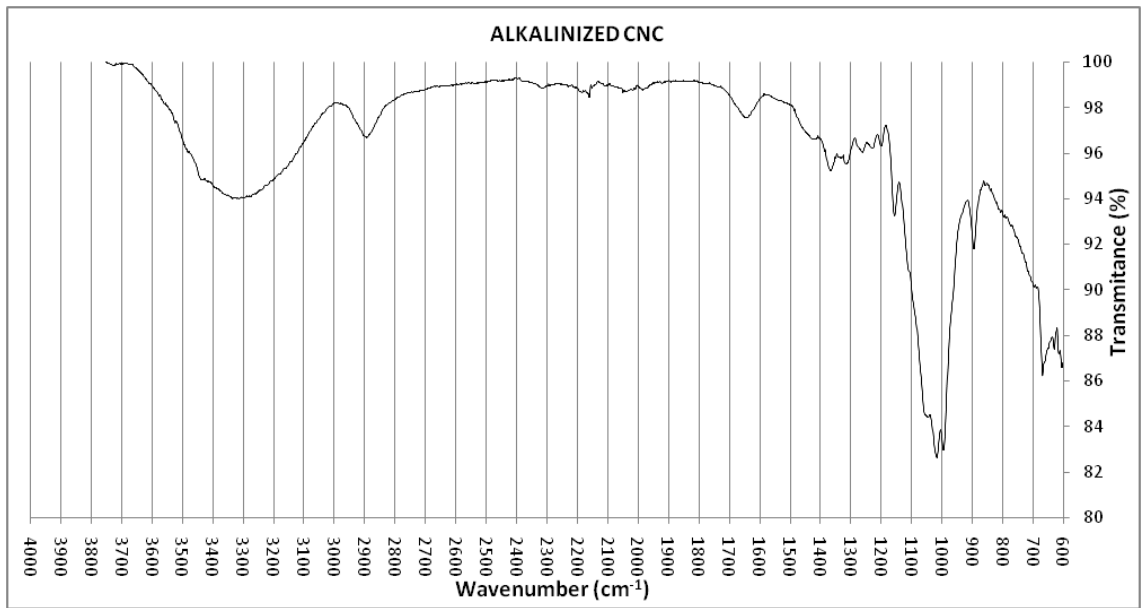Figure 20. FTIR spectra of neutralized CNC

45

Figure 21. FTIR spectra of alkalinized CNC
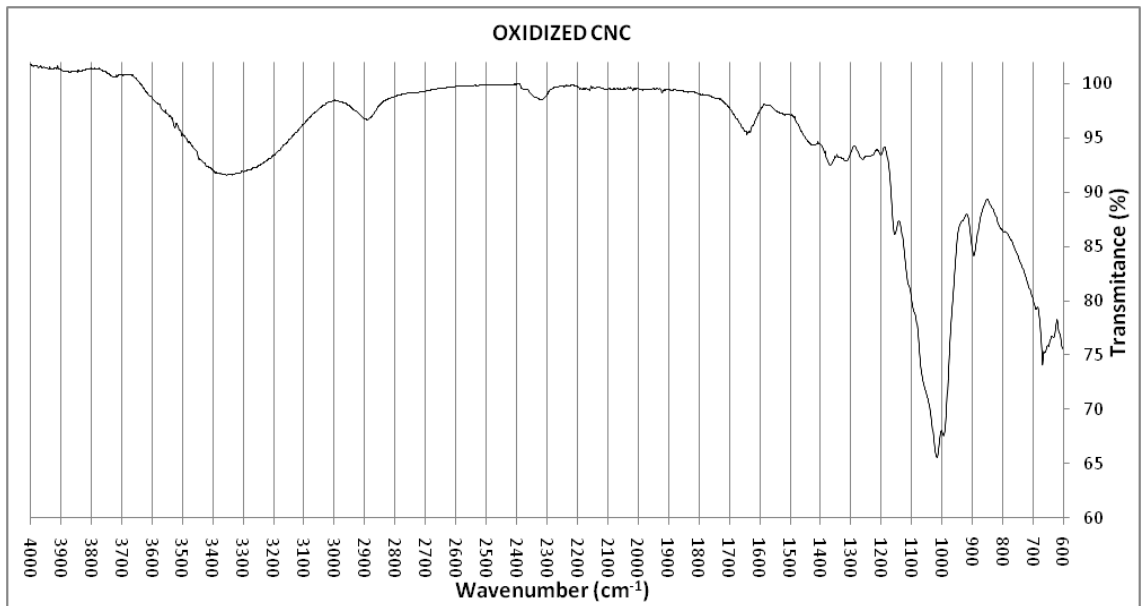
Figure 22. FTIR spectra of oxidized CNC

	Frequency (cm-1)				
Assignment	Pulp	Alkalinized CNC	Neutralized CNC	Oxidized CNC	References
combination of: cellulose O-H streching, cellulose chains intramolecular hydrogen bonds, cellulose chains intermolecular hydrogen bonds and O-H streching of weakly absorved water	broad peak 3100 - 3500	broad peak 3000 - 3600	broad peak 3000 - 3600	broad peak 3000 - 3600	[83,145,152–155]
C-H streching	2850 - 2920	2850 - 2950	2850 - 2950	2850 - 2950	[83,145,152–154]
C=O streching in: carboxylic, acetyl, ester, and uronic gropus of hemicelluloses	1750				[87,88,91,154–157]
bending vibration of cellulose adsorved water molecules	1645	1600 - 1700	1600 - 1700	1600 - 1700	[129,154,157–159]
cellulose CH2 scissoring (C6)	1425	1425	1430	1430	[129,152–155,159,160]
cellulose C-H in plane bending	1370	1370	1370	1370	[155,158,159,161]
cellulose O-H in plane bending	1345				[159–162]
cellulose CH2 wagging (C6)	1315	1315	1315	1320	[149,158–160]
OH in plane bending in polysacharides	1200	1200	1200	1200	[158,159,161,163]
asymmetric stretching of glycosidic C-O-C with contribution of: C-H in plane deformation and chain skeletal vibrations	1160	1160	1160	1160	[147,149,150,158,159,162]
asymetric in phase piranose ring streching, with contribution of: C-C streching and C-O streching	1110	1110	1110	1110	[150,158,159,163,164]
C-O streching of secondary alcohols in cellulose and C-O-C streching vibration of pyranose ring	1060	1060	1060	1060	[150,158,159,162,163]
C-O streching of cellulose primary alcohol, with contribution of: C-C streching, and cellulose C(5)-O streching	1030	1025	1025	1025	[144,158,159,162,164]
C-O streching vibration, mainly from C1 at β-glucopyranoside unit	990	995	995	995	[144,158,161,163]
band of the "anomeric region" for β-linkage (C1-H vibration coupled with C6H2 displacement)	898	895	895	895	[146–148]
out of plane bending of OH groups in polysacharides	670	670	670	670	[114,129,147,152,162]

Table 2. FTIR peak assignments for pulp and CNC spectra

3.4.4 SEM imaging

SEM images (Figures 23 to 26) of neutralized CNC are depicted featuring a morphology of agglomerated and random oriented crystals of elongated parallelepiped thin structures (resembling a blade), and nano-scale cross-section. This kind of nano structure match in form with that observed by

other authors [17,141]. The size of the crystals and the main body structure resemble those reported for cellulose type I nanocrystals, but the rounded tip match the cellulose type II crystal morphology [36,37]. A precise size determination of the obtained CNC would require the use of TEM or AFM techniques, which are out of the scope of the present work.
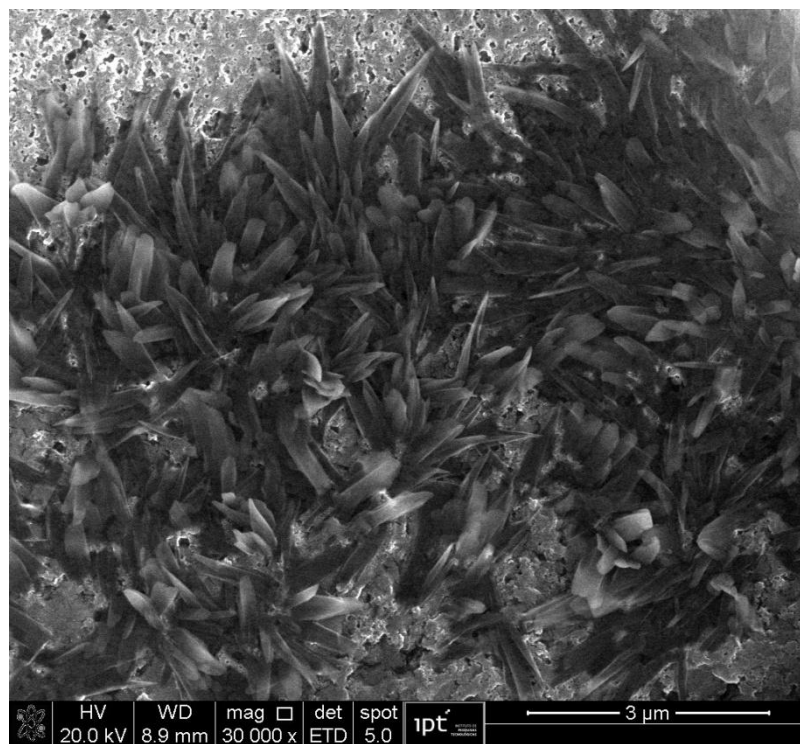
Figure 23. SEM of neutralized CNC in glass substrate
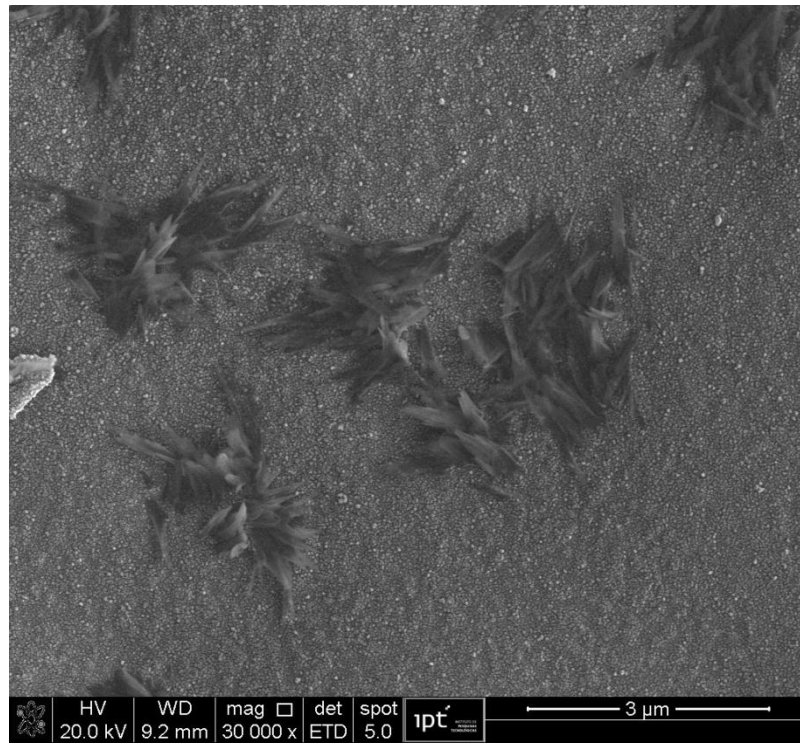
Figure 24. SEM of neutralized CNC in glass substrate
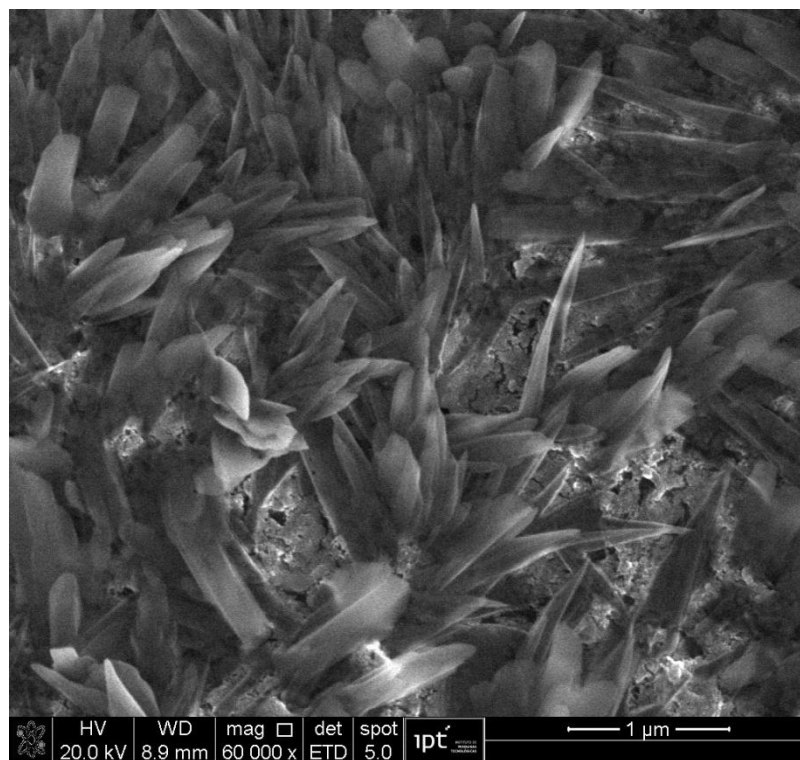
Figure 25. SEM of neutralized CNC in glass substrate
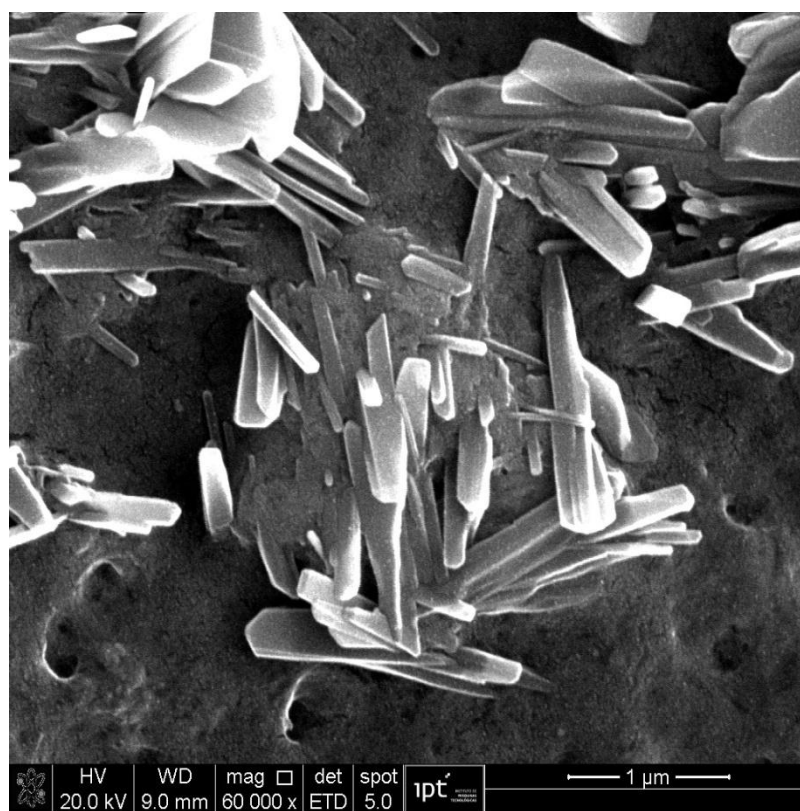
Figure 26. SEM of neutralized CNC in glass substrate

3.4.5 Cellulose nanocrystals oxidation

Dosage of potassium meta periodate (KIO_4) for oxidation require dry weight determination of CNC suspension. After the gross acid elimination following the hydrolysis, the CNC suspension maintains a small but not negligible amount of sulfuric acid in the solution. Attempts to remove water in vacuum oven (60°C, -0.84 bar) or in rotaevaporator (56°C, -0.56 bar) just remove water, leaving CNC and concentrating the sulfuric acid that promotes CNC dehydratation and charring [165]. This drawback was

overcome by neutralizing the CNC suspension as explained before. The consistency of the acid CNC suspension was 16.2 dry grams / liter.

The reaction conditions for the oxidation: periodate quantity, pH, temperature, and reaction times are the variables that control the characteristic of the product and uttermost the performance it will show when added to the paper matrix. Potassium periodate weight ratio was used in accordance with other reported experimental procedures oriented to the improvement of mechanical properties of cellulose [136,166,167]; and within the weight ratio explored in previous researches for the oxidation of CNC crystals [122] and pulp [168]. The addition of periodate was at the beginning of the reaction over the solubility limit, and that condition maintains until the end, assuring a saturation concentration (≈0.62 g/100 ml) for all the reaction length. The large excess was intended to allow besides introduction of aldehydes moieties in C2 and C3, also solubilize the amorphous cellulose still present in the suspension, due the high yield of the acid hydrolysis and the absence of a long washing step. The solubilization of cellulose due periodate oxidation occurs differentially in the amorphous and crystalline cellulose, developing faster in the first one [167]. This reaction occurs as an undesirable side reactions, due the yield loss in nanocrystals modifications [122], but as the main reaction in some procedures of nanocrystals isolation [64,130].

The CNC suspension used for the oxidation was not previously neutralized, reaching the reaction media at the beginning of the oxidation, a pH = 4. The pH affects strongly both oxidative reaction, regioselective oxidation of C2 and (reaction I in Figure 27) and also the degradative (reactions II y III in Figure 27). The kinetic analysis between hydrolysis reactions and the desired oxidation shows a close relation between both reactions, where more aldehyde content necessarily implies more hydrolysis [168]. This occurs since the oxidized glucopyranose units are more susceptible of hydrolytic attack than the unmodified (reaction II in Figure 27) [121]. Degradation increase consistently with the decrease on the pH value, and the aldehyde content reach a maximum at pH=3.5 [122,168].
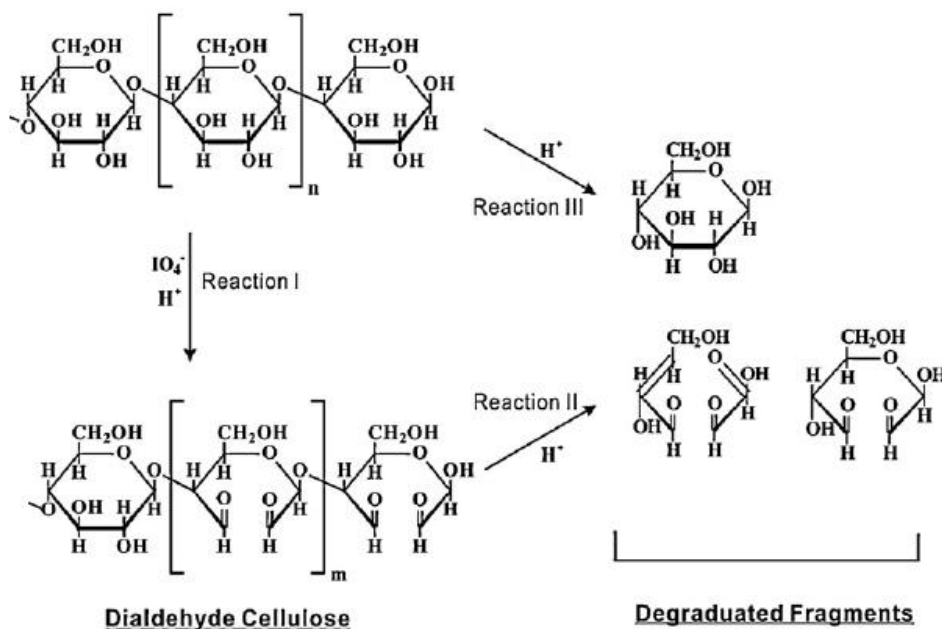
Figure 27. Oxidation and acid hydrolysis reactions of cellulose (adapted from [168])

The selected pH≈4 allows reach a good level of aldehyde groups, achieve full degradation of amorphous cellulose still present, and also avoid the use of chemicals in the pH correction. After oxidation the periodate ion reduces to iodate (IO_3^-) which in acidic media is present as iodic acid (HIO_3). This acid promotes secondary oxidations reaction with molecules liberated during the oxidative cleavage of cellulose, producing iodine as product. This was observed by the pale orange color (Figure 28) observed in the reaction baker at the end of the reaction [124]. Reaction time was according to the optimum value of 4 hours, when the maximum aldehyde content is archive, reaching this value a plateau [122,167].
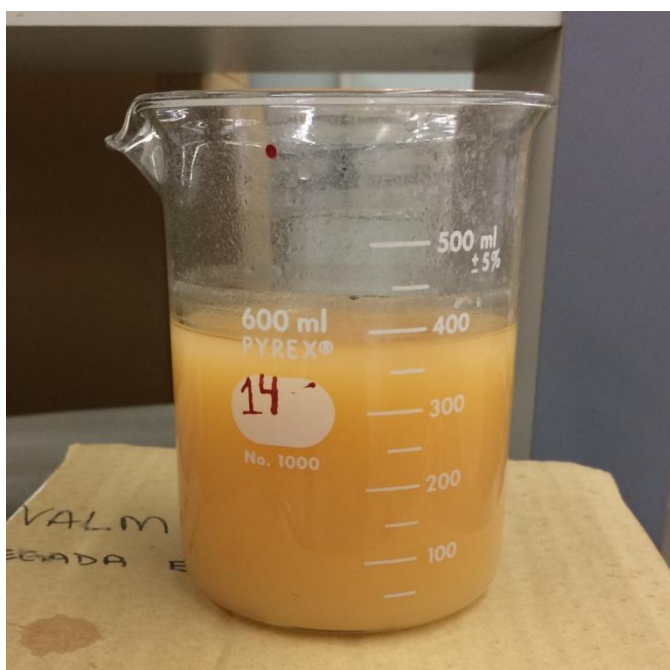
Figure 28. Reaction baker at the end of oxidation reaction

Oxidation reaction of the CNC suspension conducted at temperatures values over 40 °C produce a negligible yield due the harsh conditions of pH and periodate concentration. The selected temperature of reaction media, slightly above room temperature, is between what was reported by many authors that conduct this reaction at room temperature [64,130,136,166], and the reported optimal value of 45°C [122], and far below the temperatures (>55 °C) explored for a fast and efficient oxidation in pH neutral conditions [124]. The reaction baker was cover from light all time to avoid photo induced decomposition of aqueous periodate solution that reduce the effectiveness of the oxidant, and also to avoid the generation of free radicals species that carried unpredictable reactions with cellulose [169].

After the oxidation reaction an aliquot of the oxidized CNC suspension was repeatedly washed by centrifugation to remove chemicals. The gel like precipitated was homogeneously dispersed in a 55 mm diameter petri dish, and allowed to dry for 5 days under ambient conditions (Figure 29). The resulting film was transparent, slightly opaque, rigid and brittle. Its aspect was similar to what has been reported using others CNC film forming methods [170].
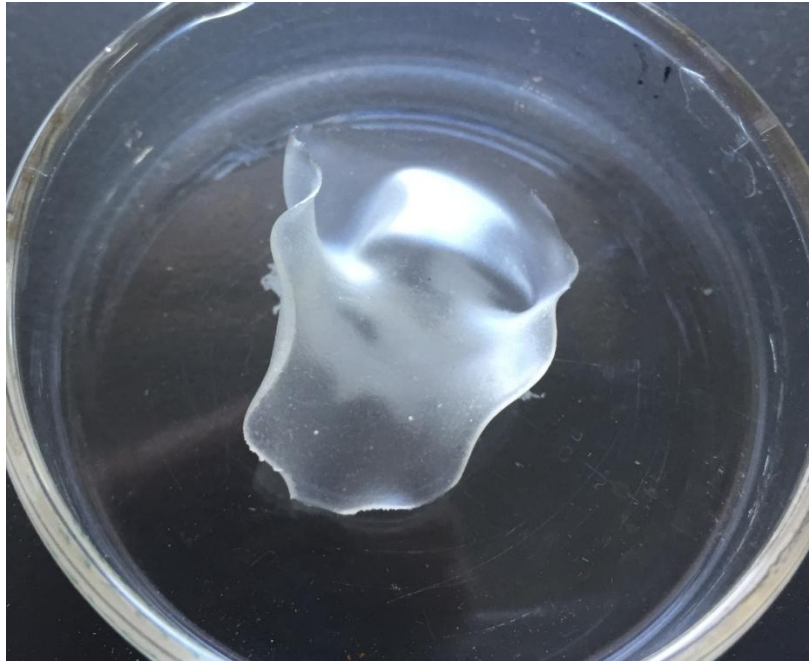
Figure 29. Oxidized CNC dried at room temperature

3.4.6 Cellulose nanocrystals alkalinization

Sulphate ester groups introduced in the cellulose nanocrystals during isolation hydrolysis grafted the surface with negative charges. In most of the reported isolation methods many of the sulphate ester groups are washed out during the long dialysis stages after hydrolysis, but in the approach of the present research dialysis washing was not used. Sulphate makes nanocrystals more soluble and probably affects negatively the retention in pulp during sheet formation. In order to evaluate this possible effect, sulfate groups was neutralized using sodium hydroxide, converting them in monosodium sulfate esters [93,109,128]. Acid CNC suspension was basified with NaOH up to pH ≈13-14, and stirred while heating during 5 hours according to the after reported method. Heating was intended to

promote hydroxyls ions diffusions to the whole bulk of cellulose crystals, but not to achieve thermal removal of sulphate groups. Despite the extreme pH conditions, removal is not expected, because higher temperatures are required to achieve cleavage of sulphate monoesters in basic aqueous solution [171]; on the contrary in slightly acidic aqueous solutions, sulfate ester groups revert to alcohol easily with a mild increase in temperature [46,50]. However, the alkaline pH conditions can prompt some modest cellulose solubilization [172].

3.4.7 Laboratory sheets formation

The refined pulp used in the sheet formation presented a Shopper-Riegel freeness value of 30.4 °SR, and the not refined 17.5 °SR. The CNC suspensions were dosed according to the addition percentage (Table 1), using as reference the solid content present in the suspension before the chemical modification (when occurred). The refined base pulp previous addition of CNC suspension presents a consistency of 32.5 % (w/w), while the not refined 46.4 % (w/w). In the case of the oxidized CNC suspension, undissolved periodate crystals were removed before dosing CNC suspension. No other treatment were completed over the modified and original CNC suspensions, like other authors reported (*eg.* liophilization or dialysis) [122,133,136]. Following this straightforward approach, none surface agent, flocculant, polyelectrolyte or any other dispersion or retention agent were used during sheet forming.

After the mixture and disaggregation stage, the pulp suspension was raised to 5.0 liters using deionized water, and the forming procedure continue according established in the standard ABNT NBR ISO 5269-1. The sheets were prepared with a basis weight of 60 g/m^2, taking into account only the base pulp amount, and do not considering the CNC added mass. The water volume used in the automatic sheet former was 8.3 liters, including the fiber suspension with CNC. It was intended that the large dilution during the forming process, and the drainage of the forming water, remove the remaining dissolved chemicals (*ie.* sulphuric acid, sodium hydroxide, and potassium periodate) from the sheet, leaving only the CNC in it. The pH value was determined in the pulp suspension in the sheet forming machine in the moment of maximum volume (8.3 liters) after the addition with 10 % of acid CNC suspension, and 10 % of alkalinized CNC suspension; the pH values were 4.0 and 10.5 respectively. Formed sheets were left to dry at room temperature for 24 hours previous conditioning.

3.4.8 Physical test of the laboratory sheets

Previous to conduct physical test, lab sheets were conditioned for 24 hours at (23 ± 1) °C and (50 ± 2) % relative humidity. In the Figures 30 to 37 are presented the values and graphs of the properties determined for each one of the lab sheet kind. The entire considerations made below about the trend exhibited by the general and mechanical properties of the

sheets, are made disregarding the expected differences that exist among the sheets, because of the natural variations in the forming process. Each sheet was manually and independently formed, and the present work did not involve such a large amount of samples to statistically obtain reliable results that allow a detailed analysis of the properties, but it was possible to observe trends.

As it can be seen in the Figure 30, the evolution of grammage in refined pulps sheets trends to increase with the addition of incremental percentages of CNC additive, maybe because the increase in mass of the CNC. The reduction in grammage showed by the refined pulps samples when the addition of 2.5 % of CNC is possibly due to the effect of basic or acid conditions over the fines generated in the refining. This effect was countered with the mass addition of the CNC. This proposal is sustained by the fact that the not refined pulp do not showed this apparent loss of mass. Nevertheless the weight gain thanks to CNC retention is expected to be more pronounced in refined pulp, because according to previous reported research the refining process generate more space for CNC adsorption [152]. Grammage increment during oxidized and alkalinized CNC addition was more significant than those of acid CNC. According the chemical nature of the different kinds of CNC, it is expected that oxidized CNC has more retention within the pulp fibers because it poses reactive aldehyde groups in C2 and C3, which can form covalent bonds with hydroxyls groups in the pulp surface or with other crystals. Alkalinized

CNC presents reduced charges in its surface, so the repulsion forces were not strong enough to ease the CNC washing during the sheet forming. For this reason CNC with high surface charges, like those of the acid suspension, are those that exhibit the poorest retention. This effect was already reported for the cellulose nanofibers addition to pulp [136]. Due to the uncertainty exhibited by the values, is possible to assert that oxidized and alkalinized CNC addition, exhibit the same behavior in all levels. On the other hand, acid CNC, composed by crystals with negative charges in the surface, and without very reactive groups on its surface, only interact with pulp surface by van der Walls forces or hydrogen bond. For this reason the refined pulp presented more retention than not refined for the acid CNC, surely because the larger exposed area per volume that naturally exhibit the refined fibers.

Grammage (g/m²)												
	0,0%			**2,5%**			**5,0%**			**10%**		
CNC + not refined pulp	61,8	±	0,1	63,1	±	0,2	63,9	±	0,2	63,7	±	0,2
CNC + refined pulp	66,3	±	0,2	62,7	±	0,1	64,7	±	0,2	65,7	±	0,2
CNC oxidized + refined pulp	66,3	±	0,2	63,9	±	0,2	64,5	±	0,2	67,6	±	0,2
CNC alkalin. + refined pulp	66,3	±	0,2	64,2	±	0,2	65,1	±	0,2	67,4	±	0,2
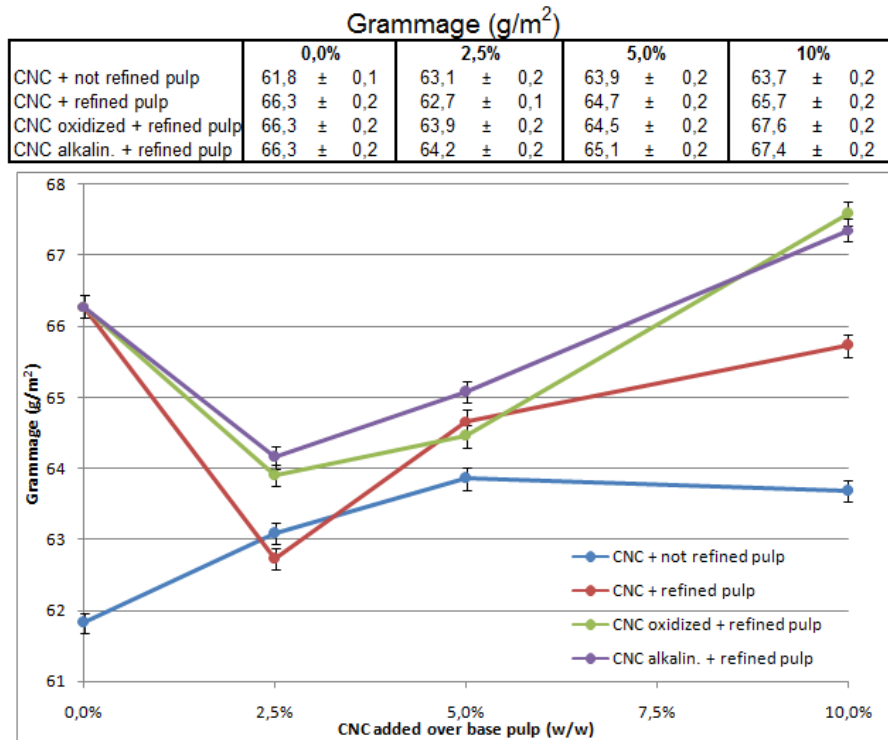
Figure 30. Grammage of laboratory sheet prepared with different kinds and amounts of CNC

Figure 31 graphs the thickness, where the observed gross difference in thickness value between refined and not refined sheets can be attributable to a more bulky fiber web characteristically formed by the latter, due the lack of fibrillation that enables fiber compaction. The thickness graphs also show a sharp reduction with the initial addition (2.5 %) and then the values stabilizes. This probably occurs because two factors: the already explained effect of basic or acid conditions over the fines generated in the refining; and the CNC addition that with its large specific area, extent the contact and fill the gaps among the fibers, promoting a better contact and thus compacting the fiber web. With the second factor one can say that a densification occurs. Should be noted that for all types of sheets, from the

2.5 % addition level onwards, considering the uncertainties of the results it is not possible to detect trends.

Thickness (mm)

	0,0%			2,5%			5,0%			10%		
CNC + not refined pulp	0,154	±	0,004	0,142	±	0,004	0,145	±	0,003	0,144	±	0,003
CNC + refined pulp	0,135	±	0,003	0,122	±	0,004	0,125	±	0,003	0,124	±	0,003
CNC oxidized + refined pulp	0,135	±	0,003	0,125	±	0,003	0,127	±	0,003	0,124	±	0,004
CNC alkalin. + refined pulp	0,135	±	0,003	0,124	±	0,004	0,128	±	0,003	0,130	±	0,003
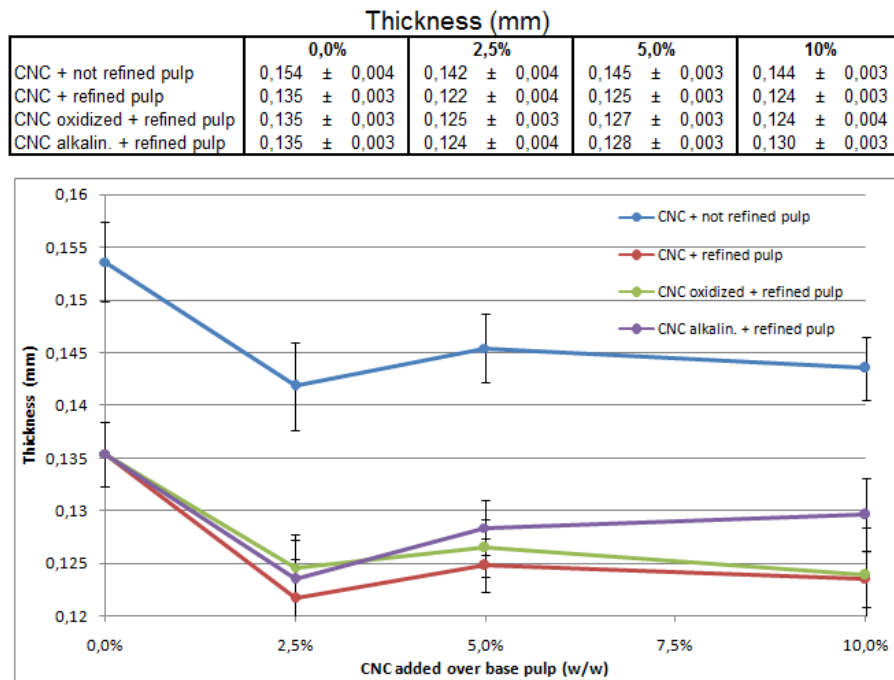
Figure 31. Thickness of laboratory sheet prepared with different kinds and amounts of CNC

The compatibility of CNC and fibers is expected, since its constituents are almost the same, so it is possible to increase the specific amount of inter fiber bonding. Considering the constant increase in grammage and that there is practically no change in thickness value, a constant decrease in the bulk of the pulp-CNC composite it is expected. As bulk is the inverse of density, it can be said that densification trend occurs, and the reason is the compaction of the fiber web due to a better contact promoted by the CNC addition, as already explain, and by the increasingly incorporation of CNC, that accommodates in the fiber surface within the web, increasing

the mass but not the volume. The bulk values are shown in Figure 32, where despite the values uncertainties, a constant decrease of bulk is observed after the initial densification.

Bulk (cm³/g)

	0,0%	2,5%	5,0%	10%
CNC + not refined pulp	2,485 ± 0,006	2,248 ± 0,005	2,277 ± 0,005	2,254 ± 0,005
CNC + refined pulp	2,043 ± 0,005	1,940 ± 0,005	1,930 ± 0,005	1,879 ± 0,005
CNC oxidized + refined pulp	2,043 ± 0,005	1,950 ± 0,005	1,963 ± 0,005	1,833 ± 0,004
CNC alkalin. + refined pulp	2,043 ± 0,005	1,925 ± 0,005	1,973 ± 0,005	1,924 ± 0,005
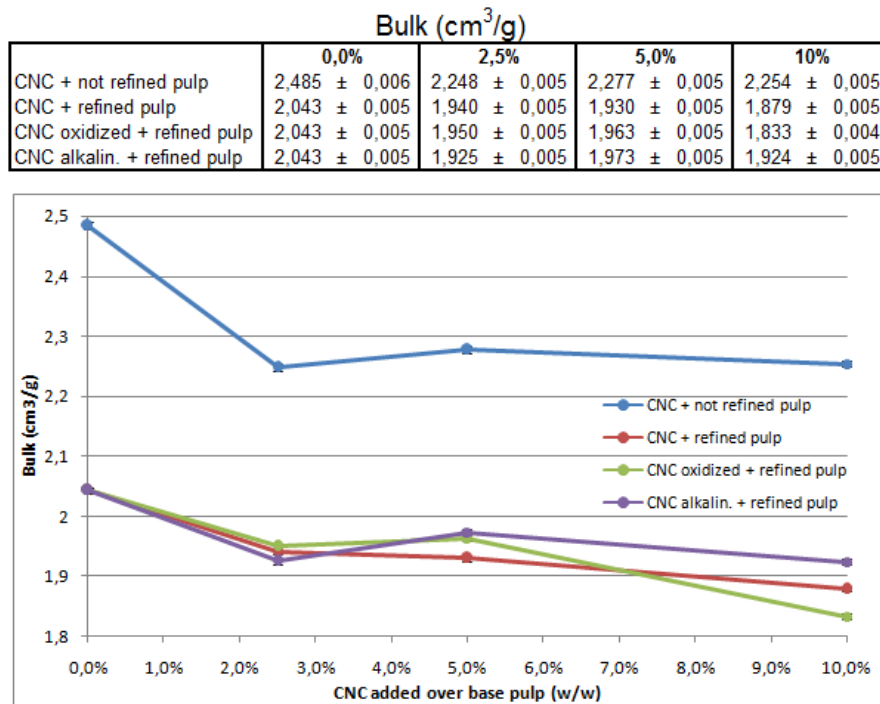
Figure 32. Bulk of laboratory sheets prepared with different kinds and amounts of CNC

The grammage increase naturally drives to an increase in the tensile strength value, so tensile index was used to permit comparison because it eliminates the influence of grammage. The incorporation of CNC that improves the contact among the elements in the fibers web has been reported as one of the reason of the improvement of mechanical properties, specially the tensile index where the bond between fibers is the governing effect [136,137]. Nevertheless the reinforcement effect resulting from the CNC addition is not explained only by the increase of the

interaction between fibers. The reported comparison of sheets made of pulp with different grades of refinement with varied density; shows that the periodate oxidized CNC supplemented paper of the same bulk exhibit superior tensile strength [136]. This effect is also observed in the behavior of the tensile index of samples with oxidized CNC in Figure 33**.** For the refined pulp samples, the initial addition of 2.5 % represents an increase in tensile strength from 24 to 32 % reaching a plateau after which subsequent addition does not promote further increase in tensile index. Taking into consideration the uncertainty of the values, all CNC types causes almost the same initial increment in value. However the 10 % addition level in oxidized CNC reflects an additional increase, reaching an incremental of 72 %. It is proposed that the initial rise obey to the densification effect, where a possible saturation effect is shown after the nanocrystal particles have promoted the coalescence of the pulp fibers. Further addition does not create new bonding; just coat fibers surface promoting a subtle increase in strength. The oxidized CNC, differs from the others kinds of CNC because posses reactive aldehyde groups on its surface capable of forming covalent bonding, hence it is possible that between addition levels 5.0 and 10 % the added amount exceeded the limit from which a continuous web of cellulose crystals bond together to have an additional reinforcement effect. This percolation effect, that has been reported in the first studies of cellulose nanocrystals composites [173], also occurs in the addition of the others CNC types, but the

reinforcement imparted by the percolation phenomenon is dependant of the strength of the union of the percolating structure, in this case cellulose nanocrystals linked by hydrogen bonding [15]. Owing to the similar chemical character of matrix and the reinforcement structure this effect is included in the coalescence effect explained before, and do not appeared as a separated phenomenon provoking a sharp improvement of tensile strength [174]. Nonetheless a mild reinforcement by percolation is observed for the not refined pulp, that increase it tensile index 35 % for 10 % addition level. In this case is possible that in the not fibrillated fibers, that does not exhibit an amount of inter fibers hydrogen bonding as large as the refined, the percolation web formed by the hydrogen bonded nanocrystals impart indeed a significant additional reinforcement. Not refined pulp with 2.5 % addition level presents a tensile index increased in 14 %, a value comparable with one reported for recycled pulp with 3 % addition of dialyzed cellulose nanocrystal, but using commercial retention and dispersion agents [133]. Previous studies have reported for periodate oxidized CNC addition, an increase of 32.6 % in tensile index with the addition of 1.2 % using retention agents [122]. This increase agreed very well with the increase of ≈32 % obtained in the present study with a 2.5 % addition of any CNC. So it is possible that this same increment in tensile index value (reach the plateau) could be achieved with smaller CNC additions amounts.

Tensile Index (N.m/g)

	0,0%			2,5%			5,0%			10%		
CNC + not refined pulp	16,91	±	1,77	19,28	±	1,33	18,78	±	1,39	22,88	±	1,71
CNC + refined pulp	38,43	±	1,19	47,68	±	2,85	48,83	±	2,95	50,22	±	1,13
CNC oxidized + refined pulp	38,43	±	1,19	50,62	±	1,52	51,81	±	2,44	66,05	±	2,68
CNC alkalin. + refined pulp	38,43	±	1,19	48,49	±	1,18	49,84	±	3,03	51,60	±	1,70
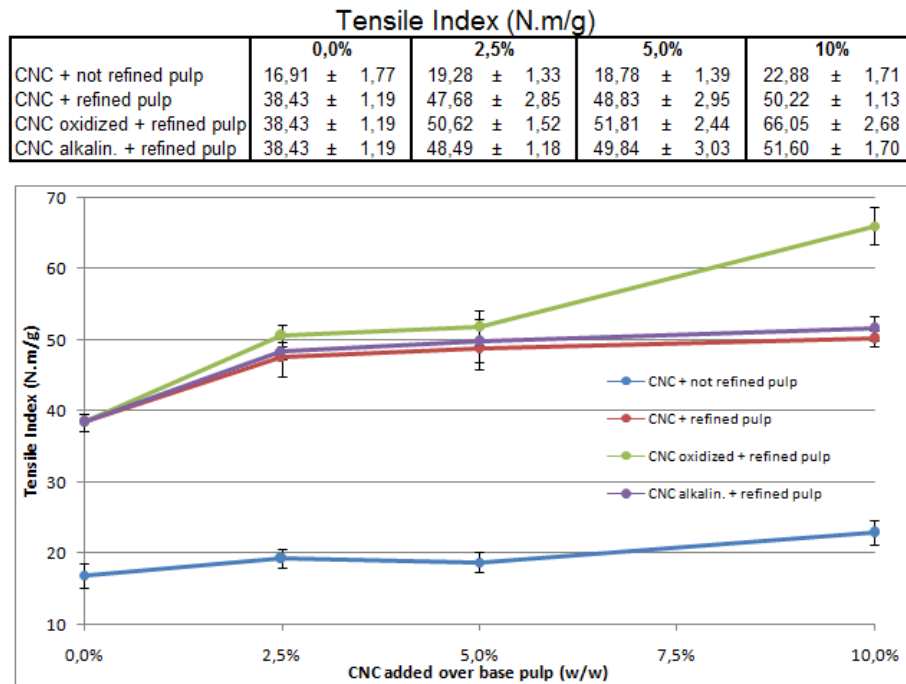
Figure 33. Tensile Index of laboratory sheet prepared with different kinds and amounts of CNC

Periodate oxidation has been reportedly used as a strategy of enhancing tear index at different structural levels. Addition of periodate oxidized CNF to pulp at 15 % without additives, has been reported to increase tensile index in 64 %, a value below the 72 % obtain in this study with a 10 % of addition [136]. Also, the direct oxidation with periodate of the fibers reaching an increase ranging from 175 to 185 % in the tensile index value has been reported [166,167].

Tear index, presented in Figure 34, exhibit a continuous improvement all along the addition levels for oxidized CNC, been the first addition level which provoke the higher increase, although with great uncertainty in all values. This increase, that is similar in value for all the CNC types, is the only significant improvement when acid and alkalinized CNC are used.

The uncertainty in values determines that alkalinized and acid CNC behave similarly, and after the initial (2.5 %) addition level, they do not exhibit further increase. The initial increase in value could be attributed to exceed the coalescence limit, in which CNC fill the gaps among fibers promoting a better bonding among them. Exceeding this addition limit, subsequent addition only acts increasing the fiber wall thickness of the fibers and their bonding contact points. This proposed mechanism is aligned with the tear strength concept, which tests the local strength of the fiber web. The work of tearing involves two concomitant processes: the stretching of fibers until breaking and the pulling out of fibers from the network. In this two process the governing factors are: the strength of individual fibers, the bonds among them, and the frictional forces between a fiber and the network [175]. Among these factors, is the strength of the individual fibers, the one that affects the most the tear index. The added CNC acts increasing the bonds among fibers, and through densification also increasing the frictional forces. In this mechanical feature, percolation is not relevant because tear resistance is a short range effect. The highest values of tear index and the major increments were for oxidized CNC; this is coherent due the fact that the reactive crystal surface is capable of forming stronger bonds. The reinforcement effect obtained for addition of acid suspension of CNC to refined pulp at 10 % was of 40 %, well above the reported 31 % of improvement obtained for addition of 15 % of bacterial nanocellulose [152].
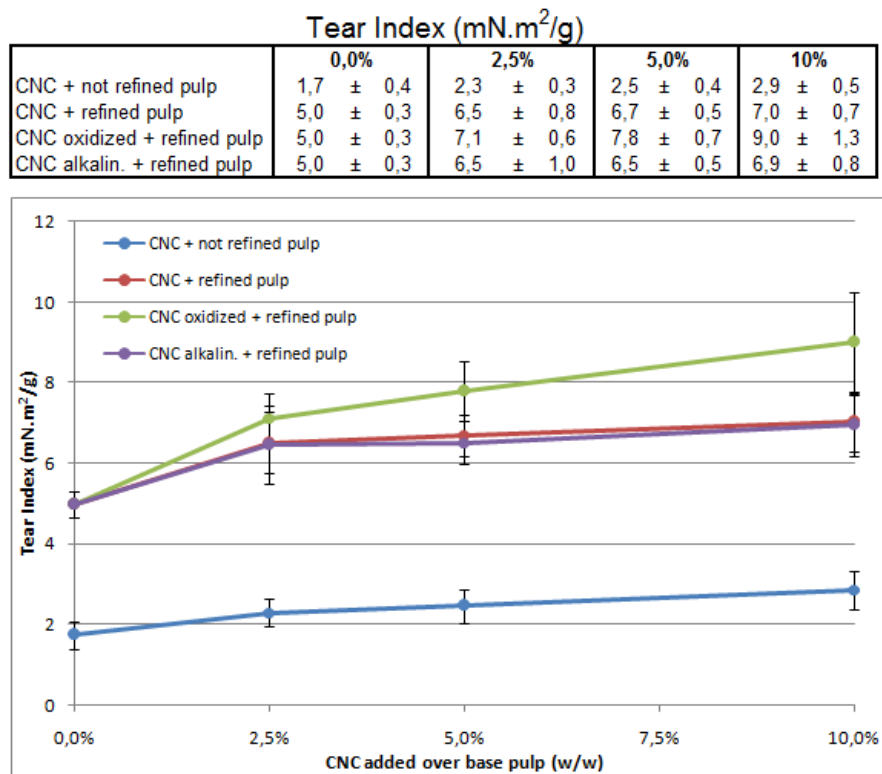
Figure 34. Tear Index of laboratory sheet prepared with different kinds and amounts of CNC

Burst index behavior presented in Figure 35, could be explained by the same propositions made for the tear index. Burst strength depends on the same factors that rule tear (mainly the strength of individual fibers, and on the bond between them), but adding the stretching capacity of the sheet [176]. The reinforcement principle observed here is the same that explained before for tear strength. The important improvement lies in the oxidized CNC addition that provokes a continuous increase in value, reaching 130 % of the base value for a 10 % addition level. This effect surely corresponds to the covalent bond forming capacity. Given the uncertainty in values, no distinctive differences are observed by the addition of acid or alkalinized CNC.

Burst Index (kPa.m²/g)	0,0%			2,5%			5,0%			10%		
CNC + not refined pulp	0,4	±	0,1	0,3	±	0,1	0,4	±	0,1	0,4	±	0,1
CNC + refined pulp	1,1	±	0,2	1,3	±	0,1	1,4	±	0,2	1,5	±	0,1
CNC oxidized + refined pulp	1,1	±	0,2	1,7	±	0,1	2,0	±	0,2	2,6	±	0,3
CNC alkalin. + refined pulp	1,1	±	0,2	1,5	±	0,2	1,4	±	0,2	1,5	±	0,2
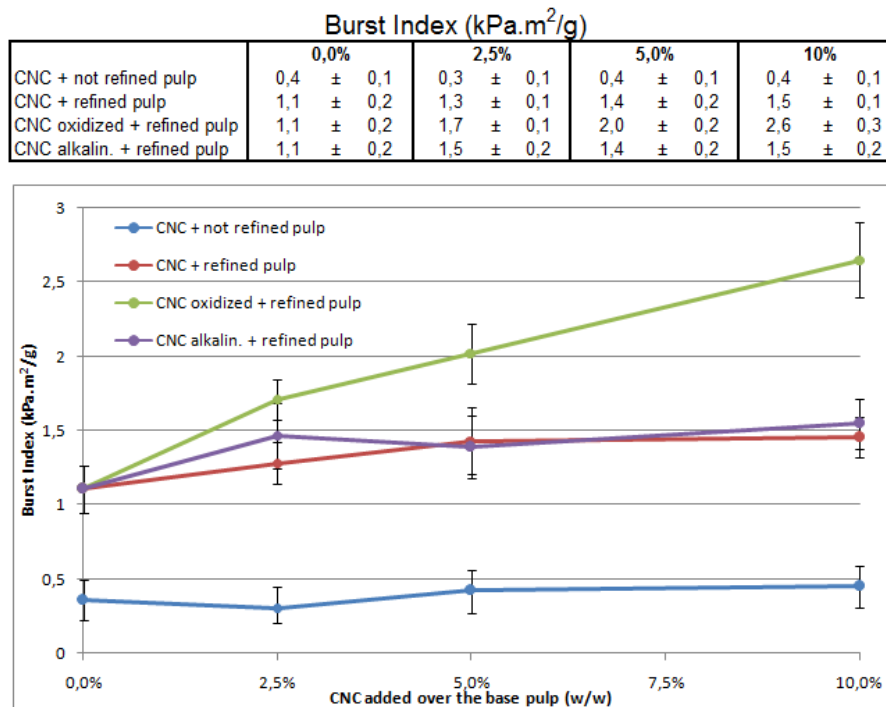
Figure 35. Burst Index of laboratory sheet prepared with different kinds and amounts of CNC

The folding endurance in Figure 36, shows a slight increase in the sheets additivated with acid CNC and alkalinized CNC, both exhibiting almost the same values. Differences in values and quantification of the degree of improvement are conditioned by the nature of this test, which is prone to results affected by a large margin of error. Nevertheless, this increase is above of reported by other authors in analogous conditions [177]. More CNC improves fiber bonding, reinforcing the fiber web and increasing the folding endurance. The oxidized CNC promotes a constant and more significant increase in value, possibly due to the stronger CNC covalent crosslink among each other and with the fibers surface. To the best knowledge of the author this mechanical parameter, has not been reported for paper supplemented with oxidized CNC. The data corresponding to the

not refined pulp with their corresponding CNC additions are not presented in the graph, because it was no possible by the method used to have a value for them.

Folding Endurance

	0,0%	2,5%	5,0%	10%
CNC + refined pulp	0,4419	0,5021	0,4919	0,6760
CNC oxidized + refined pulp	0,4419	0,7757	0,9211	1,3776
CNC alkalin. + refined pulp	0,4419	0,4919	0,6408	0,7088
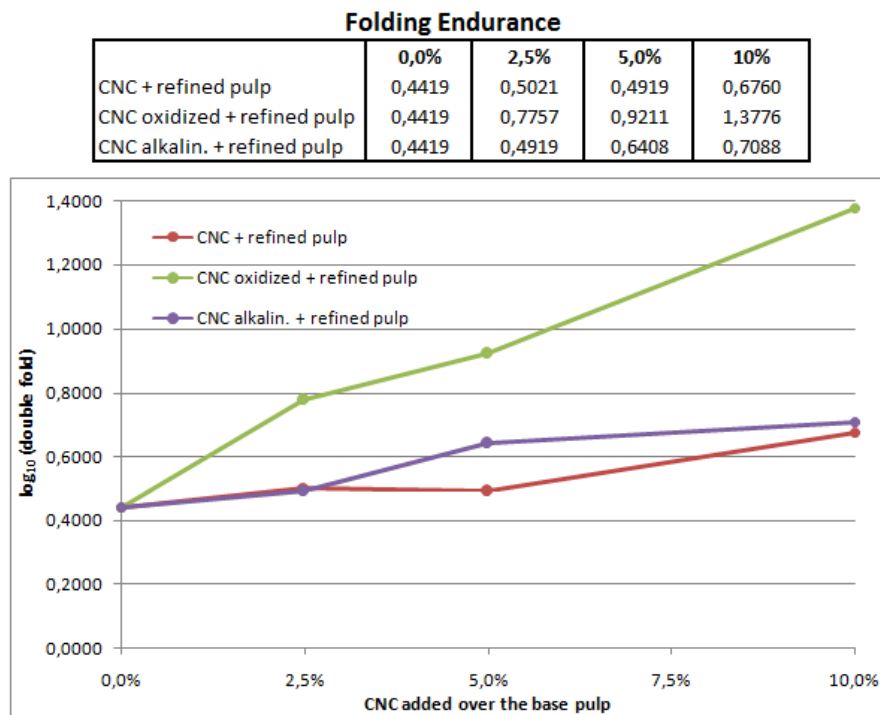
Figure 36. Folding endurance of laboratory sheet prepared with different kinds and amounts of CNC

Figure 37 shows values obtained for the air permeance property; this property depends on the number, size, shape and distribution of the pores in the paper web and it is not a mechanical property but may influence some paper converting operations such as printing, impregnation and coating. The values measured for refined pulp, showed a constant decrease with the addition of CNC. No differences are evident among the different kinds of CNC due to great uncertainty presented by the results. Despite of this, the trend clearly marks a reduction in air permeance. This

effect is coherent with the already explain phenomenon of densification having the CNC filling the pores and spaces between fibers. Similar reductions in air permeance values (mentioned as porosity in the publication) has been reported for the CNC addition in refined pulps [133].

Air Permeance µm/(Pa.s)

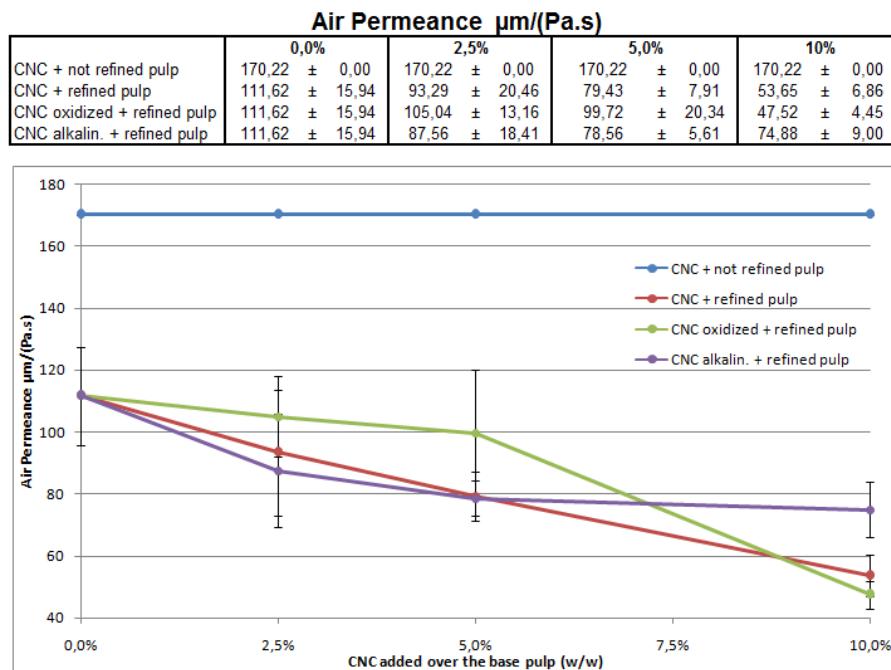|	0,0%			2,5%			5,0%			10%		
CNC + not refined pulp	170,22	±	0,00	170,22	±	0,00	170,22	±	0,00	170,22	±	0,00
CNC + refined pulp	111,62	±	15,94	93,29	±	20,46	79,43	±	7,91	53,65	±	6,86
CNC oxidized + refined pulp	111,62	±	15,94	105,04	±	13,16	99,72	±	20,34	47,52	±	4,45
CNC alkalin. + refined pulp	111,62	±	15,94	87,56	±	18,41	78,56	±	5,61	74,88	±	9,00

Figure 37. Air Permeance of laboratory sheet prepared with different kinds and amounts of CNC

3.4.9   General considerations of paper properties

A summary of the behavior of the formed sheet concerning general and mechanical properties are shown in the tables below. Table 3 detailing general properties trend, and Table 4 for the mechanical properties.

Mixture used for the sheet formation	Property			
	Grammage	Thickness	Specific volume	Air permeance
CNC acid + not refined pulp	Value increases very little with the first two additions and then remains practically constant with the final additions	Value decreases very little with the first addition and then remains practically constant with the other additions	Value decreases with the first addition and then remains practically constant with the other additions	Values are not altered by any of the addition levels
CNC acid + refined pulp	Value decreases with the first addition and then increases with the other additions	Value decreases very little with the first addition and then remains practically constant with the other additions	Value decreases very little with the first addition and then remains practically constant with the other additions	Value decrease slightly through all the additions
CNC oxidized + refined pulp	Value decreases with the first addition and then increases with the other additions	Value decreases very little with the first addition and then remains practically constant with the other additions	Value decreases very little with the first addition and then remains practically constant with the other additions	Value decrease slightly through all the additions
CNC alkalinized + refined pulp	Value decreases with the first addition and then increases with the other additions	Value decreases very little with the first addition and then remains practically constant with the other additions	Value decreases very little with the first addition and then remains practically constant with the other additions	Value decrease slightly through all the additions

Table 3. Trend of general properties

Mixture used for the sheet formation	Property			
	Tensile index	Tear index	Burst index	Folding endurance
CNC acid + not refined pulp	Value increases very little with the first addition and then remains practically constant with the other additions	Value remains practically constant through all the additions	Value remains practically constant through all the additions	For all the addition levels the resistance exhibited by the sheet was less than the minimum required to perform measurement
CNC acid + refined pulp	Value increases with the first addition and then remains practically constant with the other additions	Value increases with the first addition and then remains practically constant with the other additions	Value remains practically constant through all the additions	Value increases slightly with the addition of 10%.
CNC oxidized + refined pulp	Value increases with the first addition, being the increase significant with the addition of 10%.	Value increases continuously with the subsequent additions	Value increases continuously with the subsequent additions	Value increases continuously with the subsequent additions
CNC alkalinized + refined pulp	Value increases with the first addition and then remains practically constant with the other additions	Value increases with the first addition and then remains practically constant with the other additions	Value remains practically constant through all the additions	Value increases slightly through all the additions

Table 4. Trend of the mechanical properties

Observing Tables 3 and 4 it is possible to conclude that in non refined pulp the addition of CNCs used in this study shows any significant effect. Considering refined pulp and the general properties, it can be said that no significant effect occurred in thickness and air permeance. About grammage the effects observed was already explained in page 58. Specific volume is a value calculated from grammage and thickness, so will follow the grammage variation, once thickness shows very little

variation. Considering refined pulp and the mechanical properties it is possible to conclude that effect more significant is caused by the oxidized CNC.

The Institute for Technological Research of the State of São Paulo (IPT), Brazil, kindly provided data from sheets formed by fourteen different laboratories with the same refined pulp, of which mechanical properties were determined at IPT by the same technician. The data from IPT was compared with the ones obtained in this study for refined pulp with addition of 10 % CNC oxidized (Table 5).

Property	Values	
	Refined pulp + 10 % oxidized CNC	Refined pulp, data from IPT
Tensile index, N.m/g	66.05	44.48
Tear index, mN.m^2/g	9.0	7.7
Burst index, kPa.m^2/g	2.6	2.5

Table 5. Values obtained with oxidized CNC versus values provided by IPT.

Table 5 allows us to observe that the addition of 10 % of oxidized CNC in the refined cellulosic pulp led, respectively, to an increase of 50 % in the tensile index, 17 % in the tear index and 4 % in the burst index, in relation to the averages provided by the IPT.

3.5 Conclusions

In this study cellulose nanocrystals were successfully isolated from bleached *Eucalyptus* Kraft pulp, chemically modified, and used as reinforcement in paper, applying a straightforward approach. Long washing steps post hydrolysis, ultrasonic dispersion, purification ,addition of chemical agents usually used in the process for obtaining nanocellulose, were not applied in this study in order to better evaluate the effectiveness of a direct use of CNC. The results were a high yield isolation (≈71 % dry CNC of dry pulp), of large nanozised cellulose type II crystals with round tip blade shape. The neutralization method of sequential centrifugations, showed to be effective to an extent enough to allow CNC to cast into a translucid rigid polymer, similar to those reported by other authors that use long dialysis wash.

The use of acid and alkalinized CNC showed no relevant difference between them concerning the effect over the paper properties. However, the periodate oxidized CNC addition results in an improvement of all mechanical properties, especially Tensile Index, Burst Index and Folding Endurance. This was to our best knowledge the first time the CNC oxidation was performed using potassium periodate instead sodium periodate.

In general the observed increases is in the same order of magnitude observed by other authors, or are even better of those reported by them, using methods of preparation more complex than the used in this study.

This exploratory work proved that the fiber web can be reinforced by the addition of oxidized CNC produced in a process series easily scalable up to the industrial level. This improvement in mechanical properties was made utilizing a fully renewable additive, which starting raw material is pulp, dispensing so from additives obtained from not renewable source. Futures studies should be oriented to integrate this additive into the production of a specific type of paper were strength properties are critical (*eg.* wrapping, or tissue). The use of oxidized CNC in a pilot scale production would enable enough volume of sample to precisely evaluate the effect in those properties specifically used to measure the performance of each type of paper. And also, to evaluate the behaviors of the CNC when interacting with other components of paper (*ie.* fillers, additives, coatings, etc.), and when subjected to converting operations.

4 REFERENCES

[1]   A. Haile, G.G. Gelebo, T. Tesfaye, W. Mengie, M.A. Mebrate, A. Abuhay, D.Y. Limeneh, Bioresour. Bioprocess. 8 (2021) 35.

[2]   S. Pérez, D. Samain, Structure and Engineering of Celluloses, 2010.

[3]   P. Kumar Gupta, S. Sai Raghunath, D. Venkatesh Prasanna, P. Venkat, V. Shree, C. Chithananthan, S. Choudhary, K. Surender, K. Geetha, in: Cellulose, IntechOpen, 2019, p. 13.

[4]   G. Smook, Handbook For Pulp and Paper Technologists, Fourth Edi, TAPPI PRESS, 2016.

[5]   D.N.-S. Hon, Cellulose 1 (1994) 1–25.

[6]   J.-L. Wertz, J.P. Mercier, O. Bédué, Cellulose Science and Technology, First Edit, EPFL Press, 2010.

[7]   S.S.C. Chu, G.A. Jeffrey, Acta Crystallogr. Sect. B Struct. Crystallogr. Cryst. Chem. 24 (1968) 830–838.

[8]   R.H. Atalla, D.L. VanderHart, Solid State Nucl. Magn. Reson. 15 (1999) 1–19.

[9]   T.E. Timell, Wood Sci. Technol. 1 (1967) 45–70.

[10]   R.T. Morrison, R.N. Boyd, Organic Chemistry, 6th ed., 1992.

[11]   S. Eyley, W. Thielemans, Nanoscale 6 (2014) 7764–7779.

[12]   A.M. Donald, Encycl. Mater. Sci. Technol. (2001) 7714–7718.

[13]   Y. Nishiyama, G.P. Johnson, A.D. French, V.T. Forsyth, P. Langan, Biomacromolecules 9 (2008) 3133–3140.

[14]   A. Frey-Wyssling, Science (80-.). 119 (1954) 80–82.

[15]   M. Mariano, N. El Kissi, A. Dufresne, J. Polym. Sci. Part B Polym. Phys. 52 (2014) 791–806.

[16]   F.L. Dri, L.G. Hector, R.J. Moon, P.D. Zavattieri, Cellulose 20 (2013) 2703–2718.

[17]   W.Y. Hamad, Cellulose Nanocrystals, 2017.

[18]   K. Freudenberg, J. Chem. Educ. 9 (1932) 1171–1180.

[19]   E. Sjostrom, Wood Chemistry - Fundamentals and Applications, 2nd Editio, Academic Press, 2013.

[20]   A.C. O'Sullvian, Cellulose 4 (1997) 173–207.

[21]   K.H. Meyer, L. Misch, Helv. Chim. Acta 20 (1937) 232–244.

[22]   J. Hayashi, A. Sufoka, J. Ohkita, S. Watanabe, J. Polym. Sci. Polym. Lett. Ed. 13 (1975) 23–27.

[23]   A.D. French, G.P. Johnson, Cellulose 16 (2009) 959–973.

[24]   A.J. Stipanovic, A. Sarko, Macromolecules 9 (1976) 851–857.

[25]   Y. Nishiyama, P. Langan, H. Chanzy, J. Am. Chem. Soc. 124 (2002) 9074–9082.

[26]   Y. Nishiyama, J. Sugiyama, H. Chanzy, P. Langan, J. Am. Chem. Soc. 125 (2003) 14300–14306.

[27]   D.L. VanderHart, R.H. Atalla, Macromolecules 17 (1984) 1465–1472.

[28]   P. Chen, Y. Nishiyama, J.L. Putaux, K. Mazeau, Cellulose 21 (2014) 897–908.

[29] M. Northolt, Polymer (Guildf). 42 (2001) 8249–8264.
[30] I. Simon, L. Glasser, H.A. Scheraga, R.S.J. Manley, Macromolecules 21 (1988) 990–998.
[31] Y. Habibi, L.A. Lucia, O.J. Rojas, Chem. Rev. 110 (2010) 3479–3500.
[32] F.J. Kolpak, J. Blackwell, Macromolecules 9 (1976) 273–278.
[33] P. Langan, Y. Nishiyama, H. Chanzy, Biomacromolecules 2 (2001) 410–416.
[34] S.Y. Oh, I.Y. Dong, Y. Shin, C.K. Hwan, Y.K. Hak, S.C. Yong, H.P. Won, H.Y. Ji, Carbohydr. Res. 340 (2005) 2376–2391.
[35] S. Wang, A. Lu, L. Zhang, Prog. Polym. Sci. 53 (2016) 169–206.
[36] G. Sèbe, F. Ham-Pichavant, E. Ibarboure, A.L.C. Koffi, P. Tingaut, Biomacromolecules 13 (2012) 570–578.
[37] D.F. Martins, A.B. de Souza, M.A. Henrique, H.A. Silvério, W.P. Flauzino Neto, D. Pasquini, Ind. Crops Prod. 65 (2015) 496–505.
[38] M. Ago, T. Endo, T. Hirotsu, Cellulose 11 (2004) 163–167.
[39] J.-F. Revol, D.A.I. Goring, Polymer (Guildf). 24 (1983) 1547–1550.
[40] T. Okano, A. Sarko, J. Appl. Polym. Sci. 30 (1985) 325–332.
[41] R.F. Nickerson, J.A. Habrle, Ind. Eng. Chem. 39 (1947) 1507–1512.
[42] B.G. Rånby, Discuss. Faraday Soc. 11 (1951) 158–164.
[43] R.. Marchessault, F.. Morehead, M.J. Koch, J. Colloid Sci. 16 (1961) 327–344.
[44] D. Klemm, E.D. Cranston, D. Fischer, M. Gama, S.A. Kedzior, D. Kralisch, F. Kramer, T. Kondo, T. Lindström, S. Nietzsche, K. Petzold-Welcke, F. Rauchfuß, Mater. Today 21 (2018) 720–748.
[45] J.-F. Revol, H. Bradford, J. Giasson, R.H. Marchessault, D.G. Gray, Int. J. Biol. Macromol. 14 (1992) 170–172.
[46] P. Lu, Y. Lo Hsieh, Carbohydr. Polym. 82 (2010) 329–336.
[47] D. Trache, M.H. Hussin, M.K.M. Haafiz, V.K. Thakur, Nanoscale 9 (2017) 1763–1786.
[48] G.H.D. Tonoli, E.M. Teixeira, A.C. Corrêa, J.M. Marconcini, L.A. Caixeta, M.A. Pereira-Da-Silva, L.H.C. Mattoso, Carbohydr. Polym. 89 (2012) 80–88.
[49] M. Börjesson, G. Westman, in: Cellul. - Fundam. Asp. Curr. Trends, InTech, 2015, p. 13.
[50] S. Beck-Candanedo, M. Roman, D.G. Gray, Biomacromolecules 6 (2005) 1048–1054.
[51] E. Jin, J. Guo, F. Yang, Y. Zhu, J. Song, Y. Jin, O.J. Rojas, Carbohydr. Polym. 143 (2016) 327–335.
[52] M. Ioelovich, ISRN Chem. Eng. 2012 (2012) 1–7.
[53] J. Araki, M. Wada, S. Kuga, T. Okano, Colloids Surfaces A Physicochem. Eng. Asp. 142 (1998) 75–82.
[54] H. Sadeghifar, I. Filpponen, S.P. Clarke, D.F. Brougham, D.S. Argyropoulos, J. Mater. Sci. 46 (2011) 7344–7355.
[55] H.-Y. Yu, D.-Z. Zhang, F.-F. Lu, J. Yao, ACS Sustain. Chem. Eng. 4 (2016) 2632–2643.

[56] S. Camarero Espinosa, T. Kuhnt, E.J. Foster, C. Weder, Biomacromolecules 14 (2013) 1223–1230.

[57] L. Chen, J.Y. Zhu, C. Baez, P. Kitin, T. Elder, Green Chem. 18 (2016) 3835–3843.

[58] B. Braun, J.R. Dorgan, Biomacromolecules 10 (2009) 334–341.

[59] L. Tang, B. Huang, Q. Lu, S. Wang, W. Ou, W. Lin, X. Chen, Bioresour. Technol. 127 (2013) 100–105.

[60] Y. Liu, H. Wang, G. Yu, Q. Yu, B. Li, X. Mu, Carbohydr. Polym. 110 (2014) 415–422.

[61] P.P. Zhang, D.S. Tong, C.X. Lin, H.M. Yang, Z.K. Zhong, W.H. Yu, H. Wang, C.H. Zhou, Asia-Pacific J. Chem. Eng. 9 (2014) 686–695.

[62] H. Du, C. Liu, X. Mu, W. Gong, D. Lv, Y. Hong, C. Si, B. Li, Cellulose 23 (2016) 2389–2407.

[63] L. rong Tang, B. Huang, W. Ou, X. rong Chen, Y. dan Chen, Bioresour. Technol. 102 (2011) 10973–10977.

[64] H. Yang, D. Chen, T.G.M. van de Ven, Cellulose 22 (2015) 1743–1752.

[65] M. Visanko, H. Liimatainen, J.A. Sirviö, J.P. Heiskanen, J. Niinimäki, O. Hormi, Biomacromolecules 15 (2014) 2769–2775.

[66] A. Isogai, T. Saito, H. Fukuzumi, Nanoscale 3 (2011) 71–85.

[67] X. Cao, B. Ding, J. Yu, S.S. Al-Deyab, Carbohydr. Polym. 90 (2012) 1075–1080.

[68] A.C.W. Leung, S. Hrapovic, E. Lam, Y. Liu, K.B. Male, K.A. Mahmoud, J.H.T. Luong, Small 7 (2011) 302–305.

[69] S.R. ANDERSON, D. ESPOSITO, W. GILLETTE, J.Y. ZHU, U. BAXA, S.E. MCNEIL, TAPPI J. 13 (2014) 35–42.

[70] O. V. Surov, M.I. Voronova, N. V. Rubleva, L.A. Kuzmicheva, D. Nikitin, A. Choukourov, V.A. Titov, A.G. Zakharov, Cellulose 25 (2018) 5035–5048.

[71] X.Y. Tan, S.B. Abd Hamid, C.W. Lai, Biomass and Bioenergy 81 (2015) 584–591.

[72] H. Abushammala, I. Krossing, M.-P. Laborie, Carbohydr. Polym. 134 (2015) 609–616.

[73] L.P. Novo, J. Bras, A. García, N. Belgacem, A.A. da S. Curvelo, Ind. Crops Prod. 93 (2016) 88–95.

[74] K.N. Mohd Amin, P.K. Annamalai, I.C. Morrow, D. Martin, RSC Adv. 5 (2015) 57133–57140.

[75] W. Li, J. Yue, S. Liu, Ultrason. Sonochem. 19 (2012) 479–485.

[76] C. Weder, J.R. Capadona, K. Shanmuganathan, S. Trittschuh, S. Seidel, S.J. Rowan, C. Weder, Biomacromolecules 10 (2009) 712–716.

[77] M. Jonoobi, R. Oladi, Y. Davoudpour, K. Oksman, A. Dufresne, Y. Hamzeh, R. Davoodi, Cellulose 22 (2015) 935–969.

[78] W.H. Danial, Z. Abdul Majid, M.N. Mohd Muhid, S. Triwahyono, M.B. Bakar, Z. Ramli, Carbohydr. Polym. 118 (2015) 165–169.

[79] L. Couret, M. Irle, C. Belloncle, B. Cathala, Cellulose 24 (2017)

2125–2137.

[80] R.M.E. Sheltami, I. Abdullah, I. Ahmad, Adv. Mater. Res. 545 (2012) 119–123.

[81] B. Deepa, E. Abraham, N. Cordeiro, M. Mozetic, A.P. Mathew, K. Oksman, M. Faria, S. Thomas, L.A. Pothan, Cellulose 22 (2015) 1075–1090.

[82] B.M. Cherian, A.L. Leão, S.F. de Souza, S. Thomas, L.A. Pothan, M. Kottaisamy, Carbohydr. Polym. 81 (2010) 720–725.

[83] M.F. Rosa, E.S. Medeiros, J.A. Malmonge, K.S. Gregorski, D.F. Wood, L.H.C. Mattoso, G. Glenn, W.J. Orts, S.H. Imam, Carbohydr. Polym. 81 (2010) 83–92.

[84] S.S. Costa, J.I. Druzian, B.A.S. Machado, C.O. de Souza, A.G. Guimarães, PLoS One 9 (2014) e112554.

[85] P. Lu, Y.-L. Hsieh, Carbohydr. Polym. 87 (2012) 564–573.

[86] N. Johar, I. Ahmad, A. Dufresne, Ind. Crops Prod. 37 (2012) 93–99.

[87] A. Mandal, D. Chakrabarty, Carbohydr. Polym. 86 (2011) 1291–1299.

[88] N.S. Lani, N. Ngadi, A. Johari, M. Jusoh, J. Nanomater. 2014 (2014).

[89] G. Siqueira, J. Bras, A. Dufresne, Biomacromolecules 10 (2009) 425–432.

[90] L.A. de S. Costa, A.F. Fonsêca, F. V. Pereira, J.I. Druzian, Cellul. Chem. Technol. 49 (2015) 127–133.

[91] N.F. Mat Zain, S.M. Yusop, I. Ahmad, J. Nutr. Food Sci. 05 (2014) 10–13.

[92] M. Mariño, L. Lopes da Silva, N. Durán, L. Tasic, Molecules 20 (2015) 5908–5923.

[93] H. Kargarzadeh, I. Ahmad, I. Abdullah, A. Dufresne, S.Y. Zainudin, R.M. Sheltami, Cellulose 19 (2012) 855–866.

[94] F. Jiang, Y.-L. Hsieh, Carbohydr. Polym. 122 (2015) 60–68.

[95] J. Lamaming, R. Hashim, O. Sulaiman, C.P. Leh, T. Sugimoto, N.A. Nordin, Carbohydr. Polym. 127 (2015) 202–208.

[96] N.C. Nepomuceno, A.S.F. Santos, J.E. Oliveira, G.M. Glenn, E.S. Medeiros, Cellulose 24 (2017) 119–129.

[97] D. Pasquini, E. de M. Teixeira, A.A. da S. Curvelo, M.N. Belgacem, A. Dufresne, Ind. Crops Prod. 32 (2010) 486–490.

[98] B.M. Cherian, L.A. Pothan, T. Nguyen-Chung, G. Mennig, M. Kottaisamy, S. Thomas, J. Agric. Food Chem. 56 (2008) 5617–5627.

[99] P. Lu, Y.-L. Hsieh, Carbohydr. Polym. 87 (2012) 2546–2553.

[100] A. Barbosa, E. Robles, J. Ribeiro, R. Lund, N. Carreño, J. Labidi, Materials (Basel). 9 (2016) 1002.

[101] R. Dungani, A.F. Owolabi, C.K. Saurabh, H.P.S. Abdul Khalil, P.M. Tahir, C.I.C.M. Hazwan, K.A. Ajijolakewu, M.M. Masri, E. Rosamah, P. Aditiawati, J. Polym. Environ. 25 (2017) 692–700.

[102] D. Chen, D. Lawton, M.R. Thompson, Q. Liu, Carbohydr. Polym. 90

(2012) 709–716.

[103] E. Fortunati, F. Luzi, A. Jiménez, D.A. Gopakumar, D. Puglia, S. Thomas, J.M. Kenny, A. Chiralt, L. Torre, Carbohydr. Polym. 149 (2016) 357–368.

[104] F. Luzi, E. Fortunati, A. Jiménez, D. Puglia, D. Pezzolla, G. Gigliotti, J.M. Kenny, A. Chiralt, L. Torre, Ind. Crops Prod. 93 (2016) 276–289.

[105] F.B. de Oliveira, J. Bras, M.T.B. Pimenta, A.A. da S. Curvelo, M.N. Belgacem, Ind. Crops Prod. 93 (2016) 48–57.

[106] D. Hammiche, A. Boukerrou, H. Djidjelli, Y. Grohens, A. Bendahou, B. Seantier, J. Adhes. Sci. Technol. 30 (2016) 1899–1912.

[107] F. Kallel, F. Bettaieb, R. Khiari, A. García, J. Bras, S.E. Chaabouni, Ind. Crops Prod. 87 (2016) 287–296.

[108] W.P. Flauzino Neto, H.A. Silvério, N.O. Dantas, D. Pasquini, Ind. Crops Prod. 42 (2013) 480–488.

[109] Y. Habibi, A.L. Goffin, N. Schiltz, E. Duquesne, P. Dubois, A. Dufresne, J. Mater. Chem. 18 (2008) 5002–5010.

[110] R.J. Moon, A. Martini, J. Nairn, J. Simonsen, J. Youngblood, Chem. Soc. Rev. 40 (2011) 3941.

[111] H.P.S. Abdul Khalil, Y. Davoudpour, M.N. Islam, A. Mustapha, K. Sudesh, R. Dungani, M. Jawaid, Carbohydr. Polym. 99 (2014) 649–665.

[112] A.M.A. Gallegos, S. Herrera Carrera, R. Parra, T. Keshavarz, H.M.N. Iqbal, BioResources 11 (2016) 5641–5655.

[113] S.-P. Lin, I. Loira Calvar, J.M. Catchmark, J.-R. Liu, A. Demirci, K.-C. Cheng, Cellulose 20 (2013) 2191–2219.

[114] A. Dufresne, in: Nanocellulose, De Gruyter, Berlin, Boston, 2017.

[115] S. Eyley, W. Thielemans, Chem. Commun. 47 (2011) 4177.

[116] N. Wang, E. Ding, R. Cheng, Front. Chem. Eng. China 1 (2007) 228–232.

[117] H. Yuan, Y. Nishiyama, M. Wada, S. Kuga, Biomacromolecules 7 (2006) 696–700.

[118] M. Hasani, E.D. Cranston, G. Westman, D.G. Gray, Soft Matter 4 (2008) 2238–2244.

[119] M. de Oliveira Taipina, M.M.F. Ferrarezi, I.V.P. Yoshida, M. do C. Gonçalves, Cellulose 20 (2013) 217–226.

[120] G. Siqueira, J. Bras, A. Dufresne, Langmuir 26 (2010) 402–411.

[121] U.J. Kim, S. Kuga, M. Wada, T. Okano, T. Kondo, Biomacromolecules 1 (2000) 488–492.

[122] B. Sun, Q. Hou, Z. Liu, Y. Ni, Cellulose 22 (2015) 1135–1146.

[123] S. Coseri, G. Biliuta, B.C. Simionescu, K. Stana-Kleinschek, V. Ribitsch, V. Harabagiu, Carbohydr. Polym. 93 (2013) 207–215.

[124] A.. Varma, M.. Kulkarni, Polym. Degrad. Stab. 77 (2002) 25–27.

[125] S. Harrisson, G.L. Drisko, E. Malmström, A. Hult, K.L. Wooley, Biomacromolecules 12 (2011) 1214–1223.

[126] J. Kim, G. Montero, Y. Habibi, J.P. Hinestroza, J. Genzer, D.S.

Argyropoulos, O.J. Rojas, Polym. Eng. Sci. 49 (2009) 2054–2061.

[127] R.H. Atalla, A. Isogai, in: S. Dumitriu (Ed.), Polysaccharides Struct. Divers. Funct. Versatility, Second, CRC Press, 2004.

[128] N. Wang, E. Ding, R. Cheng, Polymer (Guildf). 48 (2007) 3486–3493.

[129] S.K. Bajpai, V. Pathak, N. Chand, B. Soni, J. Macromol. Sci. Part A Pure Appl. Chem. 50 (2013) 466–477.

[130] D. Chen, T.G.M. van de Ven, Cellulose 23 (2016) 1051–1059.

[131] C.A. Bunton, V.J. Shiner, J. Chem. Soc. (1960) 1593.

[132] N.M. Julkapli, S. Bagheri, J. Wood Sci. 62 (2016) 117–130.

[133] C. Campano, N. Merayo, A. Balea, Q. Tarrés, M. Delgado-Aguilar, P. Mutjé, C. Negro, Á. Blanco, Cellulose 25 (2018) 269–280.

[134] A. Balea, N. Merayo, E. Fuente, C. Negro, M. Delgado-Aguilar, P. Mutje, A. Blanco, Cellulose 25 (2018) 1339–1351.

[135] M. Henriksson, L.A. Berglund, P. Isaksson, T. Lindström, T. Nishino, Biomacromolecules 9 (2008) 1579–1585.

[136] R. Hollertz, V.L. Durán, P.A. Larsson, L. Wågberg, Cellulose 24 (2017) 3883–3899.

[137] T. Lindström, L. Wågberg, T. Larsson, 13th Fundam. Res. Symp. 32 (2005) 457–562.

[138] C. Miao, W.Y. Hamad, Cellulose 20 (2013) 2221–2262.

[139] M. Zeni, D. Favero, Polym. Sci. 1 (2016) 1–5.

[140] F. Camacho, P. González-Tello, E. Jurado, A. Robles, J. Chem. Technol. Biotechnol. 67 (1996) 350–356.

[141] W.Y. Hamad, T.Q. Hu, Can. J. Chem. Eng. 88 (2010) 392–402.

[142] A.D. French, Cellulose 21 (2014) 885–896.

[143] A. Thygesen, J. Oddershede, H. Lilholt, A.B. Thomsen, K. Ståhl, Cellulose 12 (2005) 563–576.

[144] S. Barsberg, J. Phys. Chem. B 114 (2010) 11703–11708.

[145] M. Åkerholm, B. Hinterstoisser, L. Salmén, Carbohydr. Res. 339 (2004) 569–578.

[146] R.G. Zhbankov, V.M. Andrianov, M.K. Marchewka, J. Mol. Struct. 436–437 (1997) 637–654.

[147] M. Mathlouthi, J.L. Koenig, Adv. Carbohydr. Chem. Biochem. 44 (1987) 7–89.

[148] M. Kacuráková, P. Capek, V. Sasinková, N. Wellner, A. Ebringerová, Carbohydr. Polym. 43 (2000) 195–203.

[149] S.D. Mansfield, E. De Jong, R.S. Stephens, J.N. Saddler, J. Biotechnol. 57 (1997) 205–216.

[150] B. Hinterstoisser, M. Åkerholm, L. Salmén, Carbohydr. Res. 334 (2001) 27–37.

[151] Q.G. Fan, D.M. Lewis, K.N. Tapley, J. Appl. Polym. Sci. 82 (2001) 1195–1202.

[152] T. Tabarsa, S. Sheykhnazari, A. Ashori, M. Mashkour, A. Khazaeian, Int. J. Biol. Macromol. 101 (2017) 334–340.

[153] V. Hospodarova, E. Singovszka, N. Stevulova, Am. J. Anal. Chem.

09 (2018) 303–310.

[154] Z. Chen, T.Q. Hu, H.F. Jang, E. Grant, Carbohydr. Polym. 127 (2015) 418–426.

[155] B. Soni, E.B. Hassan, B. Mahmoud, Carbohydr. Polym. 134 (2015) 581–589.

[156] M. Åkerholm, Dep. Fibre Polym. Technol. Doctoral (2003) 71.

[157] P. Garside, P. Wyeth, Stud. Conserv. 51 (2006) 205–211.

[158] C.M. Popescu, M.C. Popescu, G. Singurel, C. Vasile, D.S. Argyropoulos, S. Willfor, Appl. Spectrosc. 61 (2007) 1168–1177.

[159] F. Carrillo, X. Colom, J.J. Suñol, J. Saurina, Eur. Polym. J. 40 (2004) 2229–2234.

[160] M. Åkerholm, L. Salmén, Polymer (Guildf). 42 (2001) 963–969.

[161] F. Xu, J. Yu, T. Tesso, F. Dowell, D. Wang, Appl. Energy 104 (2013) 801–809.

[162] Y. Maréchal, H. Chanzy, J. Mol. Struct. 523 (2000) 183–196.

[163] M. Schwanninger, J.C. Rodrigues, H. Pereira, B. Hinterstoisser, Vib. Spectrosc. 36 (2004) 23–40.

[164] H. Chen, C. Ferrari, M. Angiuli, J. Yao, C. Raspi, E. Bramanti, Carbohydr. Polym. 82 (2010) 772–778.

[165] S. Julien, E. Chornet, R.P. Overend, J. Anal. Appl. Pyrolysis 27 (1993) 25–43.

[166] P.A. Larsson, M. Gimåker, L. Wågberg, Cellulose 15 (2008) 837–847.

[167] Q.X. Hou, W. Liu, Z.H. Liu, L.L. Bai, Ind. Eng. Chem. Res. 46 (2007) 7830–7837.

[168] X. Liu, L. Wang, X. Song, H. Song, J.R. Zhao, S. Wang, Carbohydr. Polym. 90 (2012) 218–223.

[169] M.C.R. Symons, J. Chem. Soc. (1955) 2794–2796.

[170] M. Giese, L.K. Blusch, M.K. Khan, W.Y. Hamad, M.J. Maclachlan, Angew. Chemie - Int. Ed. 53 (2014) 8880–8884.

[171] G.M. Calhoun, R.L. Burwell, J. Am. Chem. Soc. 77 (1955) 6441–6447.

[172] B. Martin-Bertelsen, E. Andersson, T. Köhnke, A. Hedlund, L. Stigsson, U. Olsson, Polymers (Basel). 12 (2020) 1–15.

[173] V. Favier, H. Chanzy, J.Y. Cavaille, Macromolecules 28 (1995) 6365–6367.

[174] M.A.S. Azizi Samir, F. Alloin, A. Dufresne, Biomacromolecules 6 (2005) 612–626.

[175] M. Ek, G. Gellerstedt, G. Henriksson, eds., Pulping Chemistry and Technology, Walter de Gruyter, Berlin, New York, 2009.

[176] E.A. Hassan, M.L. Hassan, K. Oksman, Wood Fiber Sci. 43 (2011) 76–82.

[177] V. Coccia, F. Cotana, G. Cavalaglio, M. Gelosia, A. Petrozzi, Sustainability 6 (2014) 5252–5264.